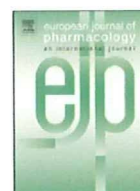


- [36] Hämäläinen A, Tervo S, Grau-Olivares M, Niskanen E, Pennanen C, Huuskonen J, et al. Voxel-based morphometry to detect brain atrophy in progressive mild cognitive impairment. *Neuroimage* 2007;37:1122–31.
- [37] Karas G, Sluimer J, Goekoop R, van der Flier W, Rombouts SA, Vrenken H, et al. Amnesic mild cognitive impairment: structural MR imaging findings predictive of conversion to Alzheimer disease. *Am J Neuroradiol* 2008;29:944–9.
- [38] Jack Jr CR, Lowe VJ, Senjem ML, Weigand SD, Kemp BJ, Shiung MM, et al. ¹¹C-PIB and structural MRI provide complementary information in imaging of Alzheimer's disease and amnesic mild cognitive impairment. *Brain* 2008;131:665–80.
- [39] McKhann G, Drachman D, Folstein M, Katzman R, Price D, Stadlan EM. Clinical diagnosis of Alzheimer's disease: report of the NINCDS-ADRDA Work Group under the auspices of Department of Health and Human Services Task Force on Alzheimer's Disease. *Neurology* 1984;34:939–44.
- [40] Petersen RC, Smith GE, Waring SC, Ivnik RJ, Tangalos EG, Kokmen E. Mild cognitive impairment: clinical characterization and outcome. *Arch Neurol* 1999;56:303–8.
- [41] Ashburner J, Friston KJ. Voxel-based morphometry—the methods. *Neuroimage* 2000;11:805–21.
- [42] Hirata Y, Matsuda H, Nemoto K, Ohnishi T, Hirao K, Yamashita F, et al. Voxel-based morphometry to discriminate early Alzheimer's disease from controls. *Neurosci Lett* 2005;382:269–74.
- [43] Pike KE, Savage G, Villemagne VL, Ng S, Moss SA, Maruff P, et al. Beta-amyloid imaging and memory in non-demented individuals: evidence for preclinical Alzheimer's disease. *Brain* 2007;130:2837–44.
- [44] Engler H, Forsberg A, Almkvist O, Blomquist G, Larsson E, Savitcheva I, et al. Two-year follow-up of amyloid deposition in patients with Alzheimer's disease. *Brain* 2006;129:2856–66.
- [45] Archer HA, Edison P, Brooks DJ, Barnes J, Frost C, Yeatman T, et al. Amyloid load and cerebral atrophy in Alzheimer's disease: an ¹¹C-PIB positron emission tomography study. *Ann Neurol* 2006;60:145–7.
- [46] Josephs KA, Whitwell JL, Ahmed Z, Shiung MM, Weigand SD, Knopman DS, et al. Beta-amyloid burden is not associated with rates of brain atrophy. *Ann Neurol* 2008;63:204–12.



Neuropharmacology and Analgesia

In vitro characterisation of BF227 binding to α -synuclein/Lewy bodies

Michelle T. Fodero-Tavoletti^{a,b,c}, Rachel S. Mulligan^f, Nobuyuki Okamura^e, Shozo Furumoto^d, Christopher C. Rowe^f, Yukitsuka Kudo^d, Colin L. Masters^c, Roberto Cappai^{a,b,c}, Kazuhiko Yanai^e, Victor L. Villemagne^{a,c,f,*}

^a Department of Pathology, The University of Melbourne, VIC, Australia

^b Bio21 Molecular and Biotechnology Institute, The University of Melbourne, VIC, Australia

^c The Mental Health Research Institute of Victoria, Tohoku University, Sendai, Japan

^d Biomedical Engineering Research Organization, Tohoku University, Sendai, Japan

^e Department of Pharmacology, Tohoku University, Sendai, Japan

^f Department of Nuclear Medicine, Austin Health, Centre for PET, VIC, Australia

ARTICLE INFO

Article history:

Received 4 March 2009

Received in revised form 6 June 2009

Accepted 22 June 2009

Available online 1 July 2009

Keywords:

BF227

α -synuclein

Positron emission tomography

Dementia with Lewy bodies

A β (amyloid- β)

Imaging

ABSTRACT

Amyloid- β (A β) plaques are a pathological hallmark of Alzheimer's disease and a current target for positron emission tomography (PET) imaging agents. Whilst [¹¹C]-PiB is currently the most widely used PET ligand in clinic, a novel family of benzoxazole compounds have shown promise as A β imaging agents; particularly BF227. We characterised the in vitro binding of [¹⁸F]-BF227 toward α -synuclein to address its selectivity for A β pathology, to establish whether [¹⁸F]-BF227 binds to α -synuclein/Lewy bodies, in addition to A β plaques. In vitro [¹⁸F]-BF227 saturation studies were conducted with 200 nM α -synuclein or A β _{1–42} fibrils or 100 μ g of Alzheimer's disease, pure dementia with Lewy bodies or control brain homogenates. Non-specific binding was established with PiB (1 μ M). In vitro binding studies indicated that [¹⁸F]-BF227 binds with high affinity to two binding sites on A β _{1–42} fibrils (K_{D1} = 1.31 and K_{D2} = 80 nM, respectively) and to one class of binding sites on α -synuclein fibrils (K_D = 9.63 nM). [¹⁸F]-BF227 bound to A β -containing Alzheimer's disease brain (K_D = 25 \pm 0.5 nM), but failed to bind to A β -free dementia with Lewy bodies or age-matched control homogenates. Moreover, BF227 labelled both A β plaques and Lewy bodies in immunohistochemical/fluorescence analysis of human Alzheimer's disease and Parkinson's disease brain sections, respectively. This study suggests that [¹⁸F]-BF227 is not A β -selective. Evaluation of BF227 as a potential biomarker for Parkinson's disease is warranted.

© 2009 Elsevier B.V. All rights reserved.

1. Introduction

Currently, there is no cure for Alzheimer's disease, an age-related neurodegenerative disease, clinically characterised by dementia. The Alzheimer's disease brain is pathologically characterised by the presence of (i) extracellular amyloid plaques comprising amyloid- β (A β); (ii) intracellular neurofibrillary tangles composed of hyperphosphorylated tau; (iii) synaptic loss and reactive gliosis; (iv) increased oxidative damage to lipids, proteins and nucleic acids and (v) bio-metal dyshomeostasis (Goedert and Spillantini, 2006).

Definitive diagnosis of Alzheimer's disease and related dementias still relies upon postmortem examination. As new therapeutic strategies

undergo clinical evaluation, considerable effort is now focused on biomarkers for the early and accurate diagnosis of Alzheimer's disease, as well as therapeutic monitoring. Modern molecular imaging procedures such as positron emission tomography (PET), may provide new insight into Alzheimer's disease by non-invasively identifying the underlying pathology of these diseases in the living. Of late, Pittsburgh compound B [PiB] has proven to be a successful biomarker for the in vivo quantitation of A β burden (Klunk et al., 2004; Rowe et al., 2007). Nonetheless, its widespread clinical use is impracticable due to the 20-minute decay half-life of carbon-11, limiting its use to centres with an on-site cyclotron. [¹⁸F]-FDDNP also highlights A β deposits in the human brain; however, FDDNP also binds to neurofibrillary tangles (Agdeppa et al., 2001), as well as PrP^{Sc} (Boxer et al., 2007; Bresjanac et al., 2003). Whilst labelling with a longer half-life isotope [¹⁸F] proves to be advantageous, FDDNP's lack of selectivity considerably reduces its ability to provide differential diagnosis of neurodegenerative diseases. Hence, the development of a specific

* Corresponding author. Department of Nuclear Medicine, Austin Health, Centre for PET 145 Studley Rd Heidelberg, VIC, 3084 Australia. Tel.: +61 3 9496 3321; fax: +61 3 9458 5023.

E-mail address: villemagne@petnm.unimelb.edu.au (V.L. Villemagne).

and selective [^{18}F]-labelled imaging agent(s) for molecular A β imaging is highly desirable to improve diagnostic accuracy and accelerate discovery and monitoring of therapeutics.

Recently, a novel series of benzoxazole compounds have been developed as PET imaging agents; namely BF227 [2-[2-(2-dimethylaminothiazol-5-yl)ethenyl]-6-[2-(fluoro)ethoxy] benzoxazole] has been demonstrated to bind to A β_{1-42} fibrils (with low nanomolar affinity) and A β plaques in Alzheimer's disease brain sections (Kudo et al., 2007). [^{11}C]-BF227-PET demonstrated retention in cerebral cortices of Alzheimer's disease patients with very little retention in normal patients; suggesting BF227 as a promising PET imaging agent for the in vivo detection of A β pathology in Alzheimer's disease patients. Whilst the specificity of BF227 binding to A β has been established, there is limited knowledge regarding its selectivity; particularly since Alzheimer's disease has been described as a 'triple brain amyloidosis' (Trojanowski, 2002), comprising A β , tau and α -synuclein that when misfolded, comprise the principal components of senile plaques, neurofibrillary tangles and Lewy bodies. Furthermore, the majority of dementia with Lewy bodies cases exhibit extensive cortical A β deposition along the pathognomonic Lewy bodies (McKeith et al., 2005). Hence, critical assessment of new radiotracers such as BF227 is warranted to avoid misinterpretation of results and/or incorrect diagnosis. Whilst BF227 binding to neurofibrillary tangles has previously been examined (Kudo et al., 2007), the potential of BF227 binding to α -synuclein has not been assessed. The aim of this study was to test the ability of BF227 to bind/recognise α -synuclein fibrils/Lewy bodies to establish whether [^{18}F]-BF227 is selective for A β pathology.

2. Materials and methods

2.1. Materials

All reagents were purchased from Sigma (St. Louis, MO), unless otherwise stated. Human A β_{1-42} was purchased from the W. M. Keck Laboratory (Yale University, New Haven, CT).

2.1.1. Tissue collection and characterisation

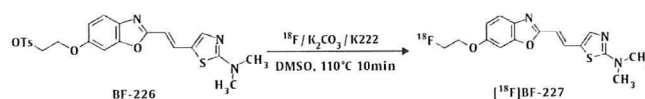
Brain tissue was collected at autopsy. The sourcing and preparation of the human brain tissue were conducted by the National Neural Tissue Resource Centre. Alzheimer's disease pathological diagnosis was made according to standard NIA-Reagan Institute criteria (1997). Dementia with Lewy bodies cases were diagnosed using consensus guidelines (McKeith et al., 1996) and classified as either dementia with Lewy bodies-A β , being subjects with evidence of neuritic plaques and/or cerebral vascular amyloid, as determined by IHC and ELISA, or pure dementia with Lewy bodies (no significant evidence of neuritic plaques and/or cerebral vascular amyloid). Parkinson's disease pathological diagnosis was made following previously described criteria (Braak et al., 2003; Forno, 1996). Determination of age-matched controls cases were also subject to the above criteria. The number of subject cases utilised is indicated in the figure/table texts. Overall, three Alzheimer's disease, three dementia with Lewy bodies-A β , one pure Dementia with Lewy bodies, two Parkinson's disease and three age-matched control subjects were utilised in this study.

2.1.2. [^{18}F] labelling of BF227

Unlabelled BF227 and 2-[2-(2-dimethylaminothiazol-5-yl)ethenyl]-6-[2-(tosyloxy)ethoxy] benzoxazole (BF-226; the precursor for [^{18}F]-BF-227) were custom synthesised by Tanabe R&D Service Co. and confirmed for purity by reverse phase high performance liquid chromatography, one dimensional NMR and mass spectrometry. [^{18}F]-BF227 was synthesised by nucleophilic substitution of the tosylate precursor (BF-226) (see below). Following a 10 min reaction at 110°C the crude reaction was partially purified on an activated Sep Pak tC18 cartridge before undergoing semi preparative reverse phase HPLC purification. Standard tC18 Sep-Pak reformulation produced [^{18}F]-BF227 in >95% radiochemical purity. The radiochemical yield was

17% (non decay corrected) and at the end of the synthesis the average specific activity was 1471 mCi/ μmol /42 GBq/ μmol .

Schematic for the radiosynthesis of [^{18}F]-BF227.



2.1.3. Preparation of amyloid fibrils

Synthetic A β_{1-42} was dissolved in 1 \times PBS pH 7.7 to a final concentration of 200 μM . Recombinant human α -synuclein was expressed and purified as previously described (Cappai et al., 2005) and dissolved in 10 mM phosphate buffer pH 7.4, to a final concentration of 200 μM . These solutions were incubated at 37°C for either 2 days for A β_{1-42} or 7 days for α -synuclein, with agitation (220 rpm, Orbital mixer incubator, Ratek). After aggregation, approximately 5% of the protein remained in the supernatant after centrifugation at 12,000 \times g for 20 minutes. Fibril aggregation was confirmed through ThT fluorescence spectroscopy and electron microscopy.

2.1.4. Preparation of human brain tissue for in vitro binding studies

Grey matter was isolated from the postmortem frontal cortex tissue from the Alzheimer's disease, dementia with Lewy bodies-A β , pure dementia with Lewy bodies and age-matched control subjects. Isolated tissue was then homogenised in 1 \times PBS (without calcium and magnesium), utilising an ultrasonic cell disrupter (2 \times 30 s, 24,000 rpm; Virsonic 600, Virtis). Protein concentration was determined using the BCA protein assay (Pierce) and brain tissue homogenates were aliquoted and frozen at -80°C until used.

2.1.5. In vitro BF227 binding assays

Synthetic A β_{1-42} or α -synuclein fibrils (200 nM) were incubated with increasing concentrations of [^{18}F]-BF227 (0.5–200 nM). To account for non-specific binding of [^{18}F]-BF227, the above mentioned reactions were duplicated in the presence of unlabelled 1 μM PiB. The binding reactions were incubated for 1 h at room temperature in 200 μl of assay buffer [PBS, minus Mg^{2+} and Ca^{2+} (JRH Biosciences, Kansas, USA); 0.1% BSA]. Binding of [^{18}F]-BF227 to human brain homogenates was assessed by incubating 100 μg brain homogenate from Alzheimer's disease, pure dementia with Lewy bodies (A β -free) and age-matched control subjects with increasing concentrations of [^{18}F]-BF227 (0.1–250nM [^{18}F]-BF227 in the absence or presence of unlabelled PiB (1 μM)), as described above. Bound from free radioactivity was separated by filtration under reduced pressure (Multi-Screen HTS Vacuum Manifold; MultiScreen HTS 96-well filtration plates; 0.65 μm , Millipore). Filters were washed three times with 200 μl assay buffer and incubated overnight in 3 ml scintillation fluid. Washed filters were assayed for radioactivity in an automatic gamma counter (Wallac 1480 Wizard 3"; Perkin Elmer). Binding data were analysed with curve fitting software that calculates the K_D and B_{max} using nonlinear regression according to the equation:

$$Y = B_{\text{max}} \cdot X$$

$$K_D + X$$

(GraphPad Prism Version 1.0, GraphPad Software, San Diego, CA). All experiments were conducted in triplicate.

2.2. Immunohistochemistry (IHC) and Fluorescence Analysis

Brain tissue from Alzheimer's disease and Parkinson's disease subjects was fixed in 10% formalin/PBS and embedded in paraffin. For immunohistochemistry and fluorescence analysis of BF227, 7 μm serial sections were assessed. Serial sections were deparaffinized and treated with 80% formic acid for 5 min and endogenous peroxidase

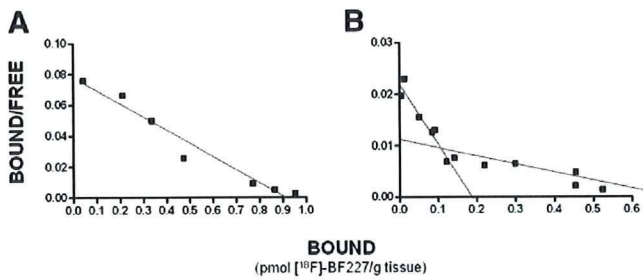


Fig. 1. In vitro binding studies indicate one class of [¹⁸F]-BF227 binding sites on α -synuclein fibrils. Scatchard plots of [¹⁸F]-BF227 binding to synthetic (A) α -synuclein or (B) A β_{1-42} fibrils. (A) Scatchard analysis identified one class of BF227 binding sites on α -synuclein fibrils (K_D of 9.63 nM and B_{max} of 2.76 pmol BF227/nmol α -synuclein). (B) Scatchard analysis identified two classes of BF227 binding sites on A β_{1-42} ; a high affinity binding site with K_D and B_{max} of 1.31 nM and 0.171 pmol BF227/nmol A β_{1-42} , respectively and a low affinity binding site with K_D and B_{max} of 80.0 nM and 2.96 pmol BF227/nmol A β_{1-42} , respectively. Binding data were analysed using GraphPad Software (Version 1.0, San Diego, CA). This figure is the average of at least three independent experiments.

activity was blocked utilising 3% hydrogen peroxide. Serial tissue sections were stained in the following order: the first and third sections were immunostained with 97/8 or 1e8 antibodies to identify Lewy bodies or A β plaques, respectively and the second section was incubated with BF227. For immunostaining, sections were treated with blocking buffer (20% fetal calf serum, 50 mM Tris-HCl, 175 mM NaCl pH 7.4) before immunostaining with primary antibodies to α -synuclein [97/8; 1:2000 dilution (Culvenor et al., 1999)] or A β (1e8; 1:50), for 1 h at room temperature. Visualisation of antibody reactivity was achieved using the LSAB™ kit (labelled streptavidin-biotin, DAKO) and sections were then incubated with hydrogen-peroxidase-diaminobenzidine (H_2O_2 -DAB) to visualise the α -synuclein or A β -positive deposits. Sections were counterstained with Mayer's hematoxylin. To assess BF227 fluorescence, quenching to minimise autofluorescence was first performed on deparaffinized tissue sections by treatment with 0.25% $KMnO_4$ /PBS for 20 min prior to washing (PBS) and incubation with 1% potassium metabisulfite/1% oxalic acid/PBS for 5 min. Following autofluorescence quenching, sections were blocked in 2% BSA/PBS pH 7.0 for 10 min and stained with 100 μ M BF227 for 30 min. Washed (PBS) sections were then mounted in non-fluorescent mounting media (DAKO). Epifluorescence images were visualised using a Zeiss microscope (47CFP; filter set 47 (EM BP 436/20, BS FT 455, EM BP480/40). Co-localisation of the BF227 and antibody signals was assessed by overlaying images from each of the stained serial tissue sections.

3. Results

3.1. Characteristics of [¹⁸F]-BF227 Binding to Recombinant α -Synuclein and A β_{1-42} Fibrils

To investigate the selectivity of BF227, we tested the ability of [¹⁸F]-BF227 to bind to synthetic α -synuclein and A β_{1-42} fibrils; the major component of Lewy bodies and senile plaques, respectively. The successful formation of fibrils was determined by ThT fluorescence and transmission electron microscopy, prior to conducting the binding assays (data not shown).

Assessment of [¹⁸F]-BF227 binding was conducted using equimolar concentrations (200 nM, $\sim 4.0 \times 10^{-11}$ mol) of either α -synuclein or A β_{1-42} fibrils. Scatchard analysis indicated that [¹⁸F]-BF227 bound to one site on α -synuclein fibrils with high affinity (K_D 9.63nM; Fig. 1A). In contrast, two classes of binding sites exist for [¹⁸F]-BF227 binding to A β_{1-42} fibrils (high affinity K_{D1} 1.31 and low affinity K_{D2} 80nM, respectively; Fig. 1B). Despite the two classes of binding sites identified for A β_{1-42} fibrils, the total number of binding sites was similar for both α -synuclein (B_{max} 2.76 pmol [¹⁸F]-BF227/nmol α -synuclein) and A β_{1-42} (B_{max1} 0.171 and B_{max2} 2.96 pmol [¹⁸F]-BF227/nmol A β_{1-42}) fibrils.

3.2. In Vitro [¹⁸F]-BF227 Binding Analysis of Human Alzheimer's Disease and Dementia With Lewy Bodies Brain

In previous studies, postmortem human brain homogenates have been extensively utilised to characterise amyloid imaging agents, including PiB (Fodero-Tavoletti et al., 2007; Klunk et al., 1995; Klunk et al., 2003; Klunk et al., 2005; Mathis et al., 2003). To further assess the selectivity of BF227, we compared the in vitro binding properties of [¹⁸F]-BF227 to A β -containing brain homogenates (Alzheimer's disease) versus A β -free (non-detectable levels of A β) homogenates (pure dementia with Lewy bodies and age-matched control). A β ELISA analysis was utilised to establish the presence/absence (non-detectable levels) of A β , prior to conducting binding studies (data not shown). [¹⁸F]-BF227 bound with high affinity to A β -containing brain homogenates. Scatchard analysis identified one class of binding sites within Alzheimer's disease homogenates with a K_D of 33 ± 4.8 nM and a B_{max} of 9353 pmol/[¹⁸F]-BF227/g tissue (Fig. 2A). In contrast, [¹⁸F]-BF227 did not bind to the α -synuclein-containing A β -free dementia with Lewy bodies (dementia with Lewy bodies-pure; Fig. 2B) or the A β - and α -synuclein-free age-matched control subjects (Fig. 2C).

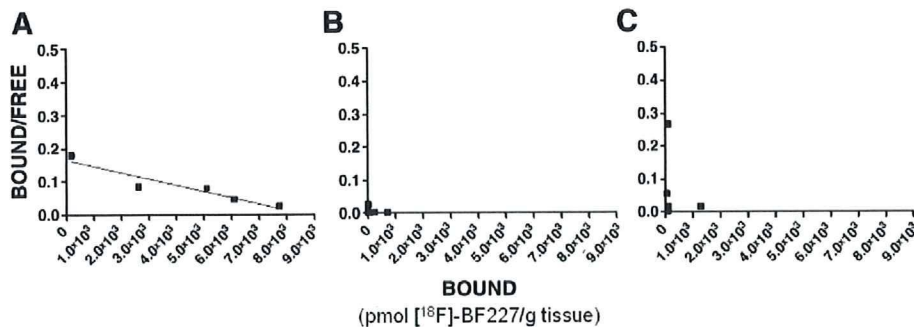


Fig. 2. In vitro binding studies demonstrate that [¹⁸F]-BF227 fails to bind to pure dementia with Lewy bodies brain homogenate. Scatchard plots of [¹⁸F]-BF227 binding to (A) AD, (B) age-matched control and (C) pure dementia with Lewy bodies brain homogenates. Scatchard analysis indicated that BF227 binds to Alzheimer's disease (K_D 33 ± 4.8 nM, B_{max} 9353 pmol/[¹⁸F]-BF227/g tissue). No significant binding of [¹⁸F]-BF227/g to pure dementia with Lewy body or age-matched control subjects was observed. Binding data were analysed using GraphPad Software (Version 1.0, San Diego, CA). This figure is the average of at least three independent experiments.

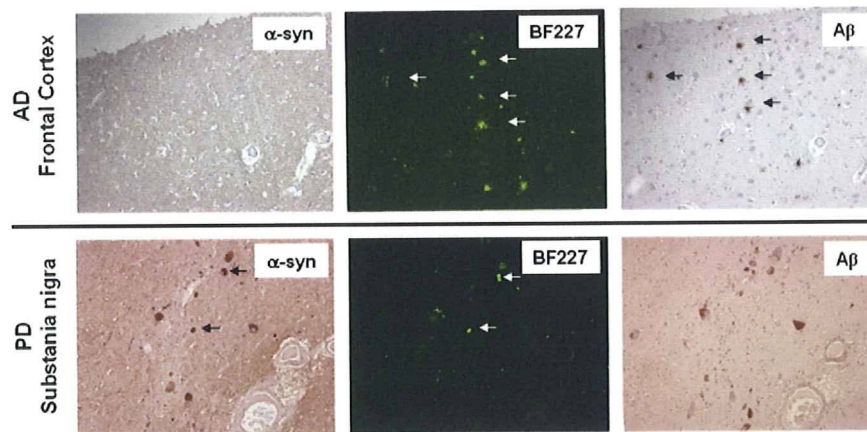


Fig. 3. Immunohistochemistry analysis indicates that BF227 binds specifically to A β plaques and not α -synuclein-containing Lewy bodies within the substantia nigra. Microscopy images of three serial sections (7 mm) from the frontal cortex of (A) Alzheimer's disease or (B) substantia nigra Parkinson's disease brain, immunostained with antibodies to α -synuclein (97/8; 1:2000) and A β (1E8; 1:50), to identify Lewy bodies and A β plaques respectively; or stained with 100 nM BF227. Black arrows indicate the location of A β plaques (top panel) and Lewy bodies (bottom panel), as determined by immunohistochemistry. White arrows indicate positive BF227 staining as detected by fluorescence, co-localising with 1E8 immunostaining of A β plaques in Alzheimer's disease subjects and Lewy bodies in the substantia nigra of Parkinson's disease subjects. Tissue sections were imaged using a Leica microscope and Axiocam digital camera. Scale bars, 50 μ m.

3.3. BF227 and Immunohistochemical Staining of Human Alzheimer's Disease and Parkinson's Disease Subjects

As a qualitative measure of its potential binding to α -synuclein deposits/Lewy bodies by fluorescence microscopy, unlabelled BF227 was used to stain fixed serial sections from the substantia nigra of Parkinson's disease subjects. Staining of the frontal cortex of Alzheimer's disease subjects was also conducted. Parkinson's disease substantia nigra sections were chosen for their rich source of Lewy bodies. BF227 staining of the substantia nigra co-localised with immuno-reactive α -synuclein-containing Lewy bodies (Fig. 3). A comparison of the α -synuclein staining Lewy bodies with BF227 staining suggested that BF227 binds to Lewy bodies as well as A β stained plaques.

4. Discussion

The ongoing quest for specific and selective PET imaging agents is imperative for the early diagnosis, treatment, development and monitoring of neurodegenerative diseases, such as Alzheimer's disease. To date, the design and testing of PET imaging candidates have suggested that compounds based on histological dyes whilst specific, are not selective for A β pathology. Benzoxazole compounds/derivatives represent a promising new family of imaging agents that may overcome some of the limitations of current PET ligands.

In vitro binding studies indicated that [18 F]-BF227 bound significantly to A β_{1-42} fibrils; exhibiting two classes of binding sites. Previous studies (Kudo et al., 2007) assessing the binding affinity of BF227 to A β_{1-42} fibrils utilised a competition binding assay that was incapable of detecting multiple classes of binding sites. This study is the first to suggest the existence of two binding sites for benzoxazole compounds on A β_{1-42} fibrils. Binding of [18 F]-BF227 to α -synuclein fibrils was observed only at an equimolar concentration to A β_{1-42} fibrils although, with a \sim 10-fold lower affinity when compared to A β_{1-42} fibrils (Fig. 1A). The lower affinity of [18 F]-BF227 for synthetic α -synuclein fibrils as compared to A β_{1-42} fibrils and the concentration of [18 F]-BF227 (\sim 1 nM) typically achieved during PET studies, suggests that the binding of [18 F]-BF227 to α -synuclein-containing Lewy bodies should not contribute significantly to the [18 F]-BF227-PET signal.

Despite the results obtained for synthetic A β_{1-42} fibrils, in vitro studies in brain homogenates failed to show two binding sites. Nevertheless, a high affinity K_D value in the low nanomolar range was observed. This distinction may reflect the fact that A β plaques are not

only composed of A β_{1-42} , but also A β_{1-40} and other longer or truncated species of A β (i.e. A β_{1-39} and A β_{1-43}) within the Alzheimer's disease brain. Despite the binding of [18 F]-BF227 to α -synuclein fibrils, no binding of [18 F]-BF227 was detected in pure dementia with Lewy bodies homogenates, devoid of A β plaques. This observation may indicate that the density of α -synuclein-containing Lewy bodies present in the pure dementia with Lewy bodies homogenates analysed may be low and therefore undetectable by [18 F]-BF227. Our previous studies assessing PiB binding to α -synuclein fibrils and pure dementia with Lewy bodies brain homogenates yielded similar results and as remarked there, the concentration of α -synuclein fibrils utilised for the in vitro studies may be physiologically unattainable, explaining the discrepancy between fibril and dementia with Lewy bodies brain homogenate results (Fodero-Tavoletti et al., 2007).

Consistent with previous reports, BF227 staining of A β plaques was clearly evident in the Alzheimer's disease brain sections examined. Fluorescence studies also demonstrated that BF227 bound to Lewy bodies, as indicated by the co-localisation of BF227 staining with α -synuclein-positive Lewy bodies (Fig. 3). Noteworthy, the concentration of BF227 used for the fluorescent studies was considerably higher (100 μ M) than the low nanomolar concentrations typically achieved during in vivo PET studies (Kudo et al., 2007).

In conclusion this study supports the notion that [18 F]-BF227 is not entirely selective for A β pathology. Whilst previous PET studies were conducted using the carbon-11 labelled BF227, we anticipate that our results would be applicable to both [11 C]- and [18 F]-labelled BF227 PET studies, as the chemical nature of BF227 is not altered using either radioisotope. Therefore, taking into consideration the calculated K_D for α -synuclein fibrils and the size and cortical density of Lewy bodies, we speculate that the potential contribution of Lewy bodies to [11 C]-BF227-PET retention in the brains of Alzheimer's disease and even dementia with Lewy bodies patients (when assessed), should be considered to be extremely low. Nevertheless, given the high affinity for α -synuclein, added to the high density of Lewy bodies in the substantia nigra of most Parkinson's disease patients, evaluation of BF227 as a Parkinson's disease diagnostic biomarker, does warrant further investigation.

Acknowledgments

The authors would like to thank Prof. Catriona McLean, Fairlie Hinton and Geoff Pavey from the National Neural Tissue Resource

Centre for sourcing and preparation of the human brain tissue. We acknowledge the funding from the National Health and Medical Research Council and Ministry of Health, Labour and Welfare, Japan. RC is an NHMRC Senior Research Fellow.

References

- Agdeppa, E.D., Kepe, V., Liu, J., Flores-Torres, S., Satyamurthy, N., Petric, A., Cole, G.M., Small, G.W., Huang, S.C., Barrio, J.R., 2001. Binding characteristics of radiofluorinated 6-dialkylamino-2-naphthylethylidene derivatives as positron emission tomography imaging probes for beta-amyloid plaques in Alzheimer's disease. *J. Neurosci.* 21, RC189.
- Boxer, A.L., Rabinovici, G.D., Kepe, V., Goldman, J., Furst, A.J., Huang, S.C., Baker, S.L., O'Neil, J.P., Chui, H., Geschwind, M.D., Small, G.W., Barrio, J.R., Jagust, W., Miller, B.L., 2007. Amyloid imaging in distinguishing atypical prion disease from Alzheimer disease. *Neurology* 69, 283–290.
- Braak, H., Del Tredici, K., Rub, U., de Vos, R.A., Jansen Steur, E.N., Braak, E., 2003. Staging of brain pathology related to sporadic Parkinson's disease. *Neurobiol. Aging* 24, 197–211.
- Bresjanac, M., Smid, L.M., Vovko, T.D., Petric, A., Barrio, J.R., Popovic, M., 2003. Molecular-imaging probe 2-(1-[6-(2-fluoroethyl)(methyl) amino]-2-naphthyl]ethylidene) malononitrile labels prion plaques in vitro. *J. Neurosci.* 23, 8029–8033.
- Cappai, R., Leck, S.L., Tew, D.J., Williamson, N.A., Smith, D.P., Galatis, D., Sharples, R.A., Curtain, C.C., Ali, F.E., Cherny, R.A., Culvenor, J.G., Bottomley, S.P., Masters, C.L., Barnham, K.J., Hill, A.F., 2005. Dopamine promotes alpha-synuclein aggregation into SDS-resistant soluble oligomers via a distinct folding pathway. *FASEB. J.* 19, 1377–1379.
- Culvenor, J.G., McLean, C.A., Cutt, S., Campbell, B.C., Maher, F., Jakala, P., Hartmann, T., Beyreuther, K., Masters, C.L., Li, Q.X., 1999. Non-Abeta component of Alzheimer's disease amyloid (NAC) revisited. NAC and alpha-synuclein are not associated with Abeta amyloid. *Am. J. Pathol.* 155, 1173–1181.
- Fodero-Tavoletti, M.T., Smith, D.P., McLean, C.A., Adlard, P.A., Barnham, K.J., Foster, L.E., Leone, L., Perez, K., Cortes, M., Culvenor, J.G., Li, Q.X., Laughton, K.M., Rowe, C.C., Masters, C.L., Cappai, R., Villemagne, V.L., 2007. In vitro characterization of Pittsburgh compound-B binding to Lewy bodies. *J. Neurosci.* 27, 10365–10371.
- Forno, L.S., 1996. Neuropathology of Parkinson's disease. *J. Neuropathol. Exp. Neurol.* 55, 259–272.
- Goedert, M., Spillantini, M.G., 2006. A century of Alzheimer's disease. *Science (New York, N.Y.)* 314, 777–781.
- Klunk, W.E., Debnath, M.L., Pettegrew, J.W., 1995. Chrysin-G binding to Alzheimer and control brain: autopsy study of a new amyloid probe. *Neurobiol. Aging* 16, 541–548.
- Klunk, W.E., Engler, H., Nordberg, A., Bacskai, B.J., Wang, Y., Price, J.C., Bergstrom, M., Hyman, B.T., Langstrom, B., Mathis, C.A., 2003. Imaging the pathology of Alzheimer's disease: amyloid-imaging with positron emission tomography. *Neuroimaging Clinics of North America* 13, 781–789, ix.
- Klunk, W.E., Engler, H., Nordberg, A., Wang, Y., Blomqvist, G., Holt, D.P., Bergstrom, M., Savitcheva, I., Huang, G.F., Estrada, S., Ausen, B., Debnath, M.L., Barletta, J., Price, J.C., Sandell, J., Lopresti, B.J., Wall, A., Koivisto, P., Antoni, G., Mathis, C.A., Langstrom, B., 2004. Imaging brain amyloid in Alzheimer's disease with Pittsburgh compound-B. *Ann. Neurol.* 55, 306–319.
- Klunk, W.E., Lopresti, B.J., Ikonovic, M.D., Lefterov, I.M., Koldamova, R.P., Abrahamson, E.E., Debnath, M.L., Holt, D.P., Huang, G.F., Shao, L., DeKosky, S.T., Price, J.C., Mathis, C.A., 2005. Binding of the positron emission tomography tracer Pittsburgh compound-B reflects the amount of amyloid-beta in Alzheimer's disease brain but not in transgenic mouse brain. *J. Neurosci.* 25, 10598–10606.
- Kudo, Y., Okamura, N., Furumoto, S., Tashiro, M., Furukawa, K., Maruyama, M., Itoh, M., Iwata, R., Yanai, K., Arai, H., 2007. 2-(2-[2-Dimethylaminothiazol-5-yl]ethenyl)-6-(2-[fluoro]ethoxy)benzoxazole: a novel PET agent for in vivo detection of dense amyloid plaques in Alzheimer's disease patients. *J. Nucl. Med.* 48, 553–561.
- Mathis, C.A., Wang, Y., Holt, D.P., Huang, G.F., Debnath, M.L., Klunk, W.E., 2003. Synthesis and evaluation of 11C-labeled 6-substituted 2-arylbenzothiazoles as amyloid imaging agents. *J. Medicinal. Chem.* 46, 2740–2754.
- McKeith, I.G., Dickson, D.W., Lowe, J., Emre, M., O'Brien, J.T., Feldman, H., Cummings, J., Duda, J.E., Lippa, C., Perry, E.K., Aarsland, D., Arai, H., Ballard, C.G., Boeve, B., Burn, D.J., Costa, D., Del Ser, T., Dubois, B., Galasko, D., Gauthier, S., Goetz, C.G., Gomez-Tortosa, E., Halliday, G., Hansen, L.A., Hardy, J., Iwatsubo, T., Kalaria, R.N., Kaufer, D., Kenny, R.A., Krczyn, A., Kosaka, K., Lee, V.M., Lees, A., Litvan, I., Londos, E., Lopez, O.L., Minoshima, S., Mizuno, Y., Molina, J.A., Mukaetova-Ladinska, E.B., Pasquier, F., Perry, R.H., Schulz, J.B., Trojanowski, J.Q., Yamada, M., 2005. Diagnosis and management of dementia with Lewy bodies: third report of the DLB Consortium. *Neurology* 65, 1863–1872.
- McKeith, I.G., Galasko, D., Kosaka, K., Perry, E.K., Dickson, D.W., Hansen, L.A., Salmon, D.P., Lowe, J., Mirra, S.S., Byrne, E.J., Lennox, G., Quinn, N.P., Edwardson, J.A., Ince, P.G., Bergeron, C., Burns, A., Miller, B.L., Lovestone, S., Collerton, D., Jansen, E.N., Ballard, C., de Vos, R.A., Wilcock, G.K., Jellinger, K.A., Perry, R.H., 1996. Consensus guidelines for the clinical and pathologic diagnosis of dementia with Lewy bodies (DLB): report of the Consortium on DLB International Workshop. *Neurology* 47, 1113–1124.
- Rowe, C.C., Ng, S., Ackermann, U., Gong, S.J., Pike, K., Savage, G., Cowie, T.F., Dickinson, K.L., Maruff, P., Darby, D., Smith, C., Woodward, M., Merory, J., Tochon-Danguy, H., O'Keefe, G., Klunk, W.E., Mathis, C.A., Price, J.C., Masters, C.L., Villemagne, V.L., 2007. Imaging beta-amyloid burden in aging and dementia. *Neurology* 68, 1718–1725.
- Trojanowski, J.Q., 2002. Emerging Alzheimer's disease therapies: focusing on the future. *Neurobiol. Aging* 23, 985–990.

A traditional medicinal herb *Paeonia suffruticosa* and its active constituent 1,2,3,4,6-penta-*O*-galloyl- β -D-glucopyranose have potent anti-aggregation effects on Alzheimer's amyloid β proteins *in vitro* and *in vivo*

Hironori Fujiwara,* Masahiro Tabuchi,† Takuji Yamaguchi,† Koh Iwasaki,* Katsutoshi Furukawa,‡ Kyoji Sekiguchi,† Yasushi Ikarashi,† Yukitsuka Kudo,§ Makoto Higuchi,¶,** Takaomi C. Saido,** Sumihiro Maeda,†† Akihiko Takashima,†† Masahiko Hara,‡‡ Nobuo Yaegashi,* Yoshio Kase† and Hiroyuki Arai‡

*Center for Asian Traditional Medicine, Tohoku University Graduate School of Medicine, Sendai, Aoba-ku, Japan

†TSUMURA Research Laboratories, TSUMURA & Co., Ibaraki, Japan

‡Department of Geriatrics and Gerontology, Division of Brain Sciences, Institute of Development, Aging and Cancer, Tohoku University, Aoba-ku, Sendai, Japan

§Innovation of Biomedical Engineering Center, Tohoku University, Aoba-ku, Sendai, Japan

¶Molecular Imaging Center, National Institute of Radiological Sciences, Inage-ku, Chiba, Japan

**Laboratory for Proteolytic Neuroscience, RIKEN Brain Science Institute, Wako, Saitama, Japan

††Laboratory for Alzheimer's Disease, RIKEN Brain Science Institute, Wako, Saitama, Japan

‡‡Local Spatio-Temporal Functions Laboratory, RIKEN Frontier Research System, Wako, Saitama, Japan

Abstract

The deposition of amyloid β (A β) protein is a consistent pathological hallmark of Alzheimer's disease (AD) brains; therefore, inhibition of A β fibril formation and destabilization of pre-formed A β fibrils is an attractive therapeutic and preventive strategy in the development of disease-modifying drugs for AD. This study demonstrated that *Paeonia suffruticosa*, a traditional medicinal herb, not only inhibited fibril formation of both A β _{1–40} and A β _{1–42} but it also destabilized pre-formed A β fibrils in a concentration-dependent manner. Memory function was examined using the passive-avoidance task followed by measurement of A β burden in the brains of Tg2576 transgenic mice. The herb improved long-term memory impairment in the transgenic mice and inhibited the accumulation of A β in the brain. Three-dimensional HPLC

analysis revealed that a water extract of the herb contained several different chemical compounds including 1,2,3,4,6-penta-*O*-galloyl- β -D-glucopyranose (PGG). No obvious adverse/toxic were found following treatment with PGG. As was observed with *Paeonia suffruticosa*, PGG alone inhibited A β fibril formation and destabilized pre-formed A β fibrils *in vitro* and *in vivo*. Our results suggest that both *Paeonia suffruticosa* and its active constituent PGG have strong inhibitory effects on formation of A β fibrils *in vitro* and *in vivo*. PGG is likely to be a safe and promising lead compound in the development of disease-modifying drugs to prevent and/or cure AD.

Keywords: 1,2,3,4,6-penta-*O*-galloyl- β -D-glucopyranose, Alzheimer's disease, amyloid β protein, medicinal herb, *Paeonia suffruticosa*, Tg2576 transgenic mice.

J. Neurochem. (2009) **109**, 1648–1657.

Received November 27, 2008; revised manuscript received March 10, 2009; accepted March 23, 2009.

Address correspondence and reprint requests to Hiroyuki Arai, M.D., Ph.D., Department of Geriatrics and Gerontology, Division of Brain Sciences, Institute of Development, Aging and Cancer, Tohoku University, 4-1 Seiryō-cho Aobaku, Sendai 980-8575, Japan.
E-mail: harai@idac.tohoku.ac.jp

Abbreviations used: AD, Alzheimer's disease; APP, amyloid precursor protein; A β , amyloid β ; MTT, 3-(4,5-dimethylthiazol-2-yl)-2,5-diphenyltetrazolium bromide; PGG, 1,2,3,4,6-penta-*O*-galloyl- β -D-glucopyranose.

Alzheimer's disease (AD) is the most prevalent cause of dementia and is characterized by loss of memory and cognition as well as behavioral and occupational instability in old age. One of the pathological characteristics of AD is the progressive deposition of insoluble amyloid β protein (A β) as a form of senile plaques (Wirhns *et al.* 2004). This protein comprises peptides of approximately 39 to 43 amino acid residues derived from the transmembrane amyloid precursor protein (APP) (Selkoe 2002). A β can form monomers and a variety of different aggregate morphologies including dimers, small soluble oligomers, protofibrils, diffuse plaques, and fibrillar deposits seen in the senile plaques. Protofibrils, diffuse plaques, and fibrillar deposits seem to have a predominant β -sheet structure (Tierney *et al.* 1988; Barrow and Zagorski 1991), while oligomers are believed to be more globular (Barghorn *et al.* 2005). Increasing evidence that the formation of these aggregates, particularly oligomer, causes primary neurodegeneration in AD has led to the amyloid hypothesis which states that the accumulation of A β in the CNS is highly neurotoxic and deteriorates synaptic functions (Selkoe 2002; Wirhns *et al.* 2004). Moreover, several lines of evidence suggest that A β accumulation begins at relatively early stages before cognitive decline becomes manifest (Anderton *et al.* 1998; Selkoe 2002). Therefore, it is hypothesized that the formation, deposition, and aggregation of A β in the brain should be primary targets for complete amelioration of dementia. Currently, drugs available for dementia such as acetylcholinesterase inhibitors exert only a temporary benefit on cognitive dysfunction (Millard and Broomfield 1995; Park *et al.* 2000; Darreh-Shori *et al.* 2004), and they do not prevent or reverse the formation of A β deposits. One potentially promising strategy for developing more effective anti-dementia drugs is the inhibition of A β fibril formation or destabilization of aggregated A β or a combination of both.

Herbal remedies are used worldwide and have a long history of use in alleviating a variety of symptoms of many different conditions and diseases. Recently, clinical trials in AD patients have also shown that some of these traditional medications improved Mini-Mental State Examination scores, P300 latency, and blood flow in the cerebral cortex (Le Bars *et al.* 1997). Although inconclusive, these provocative studies suggest that even old remedies can be beneficial in AD and related disorders. We have reported that several traditional herbal medicines such as *Formula lienalis angelicae compositae* (kamiuntanto) (Suzuki *et al.* 2001; Nakagawasai *et al.* 2004), *Pilulae octo-medicamentorum rehmanniae* (hachimijogan) (Iwasaki *et al.* 2004), and *Pulvis depressionis hepatis* (yokukansan) (Iwasaki *et al.* 2005) improved symptoms of dementia. The radice cortex of *Paeonia suffruticosa* (*Moutan cortex*; Botan-pi), a major medicinal plant comprising *Pilulae octo-medicamentorum rehmanniae*, is used as an anti-pyretic and anti-inflammatory agent (Lin *et al.* 1999; Yasuda *et al.* 1999; Chou 2003).

Paeonol, a common component of *Paeonia suffruticosa*, has been shown to inhibit platelet aggregation in rabbits (Lin *et al.* 1999) as well as to reduce cerebral infarction in ischemia-reperfusion-injured rats (Hsieh *et al.* 2006). However, the underlying mechanism of traditional medicinal herbs, including *Paeonia suffruticosa*, on the formation and metabolism of A β fibrils has never been investigated. In the present study, we examined the effect of *Paeonia suffruticosa* on the formation of A β aggregates and its ability to destabilize pre-formed A β fibrils *in vitro* by using fluorescence spectroscopy with thioflavin T.

1,2,3,4,6-Penta-*O*-galloyl- β -D-glucopyranose (PGG), a high molecular weight tannin-type polyphenols, has been isolated from *Paeonia suffruticosa*. The defining characteristic of tannins is their ability to bind and precipitate proteins (Hofmann *et al.* 2006). Li *et al.* (2005) previously reported that PGG could bind to insulin receptors and activate an insulin-mediated glucose transport signaling pathway. However, the effect of this compound on the formation and metabolism of A β fibrils has not yet been investigated.

Our results provide strong evidence that several traditional herbs extracts including *Paeonia suffruticosa* and PGG have inhibitory and destabilizing effects on A β fibrils.

Materials and methods

Reagents

A β peptides (1–40 and 1–42) and thioflavin-T were obtained from Peptide Institute (Osaka, Japan) and from Sigma (St Louis, MO, USA), respectively. All the reagents and drugs used were of analytical grade.

Preparation of medicinal herb extracts

Water, 100% methanol, and 99.5% ethanol extracts of medicinal herbs were prepared by refluxing 10 g of sliced dry herbs in 100 mL of each solution for 30 min. The decoction after cooling to 25°C was evaporated completely under reduced pressure to yield dried or oily extracts. The extracts were weighed and dissolved in dimethylsulfoxide at a concentration of 100 mg/mL and then stored at –20°C. When assaying, these extracts were dissolved in 50 mM potassium phosphate buffer (pH 7.4) and the solutions were adjusted to pH 7.4 when necessary.

Analysis of three-dimensional HPLC fingerprints of water extract of *Paeonia suffruticosa*

Paeonia suffruticosa (0.5 g) was extracted with 30 mL of distilled water under ultrasonication for 30 min. The solution was filtered and then analyzed by HPLC. The HPLC system consisted of an HPLC pump (LC-10AD; Shimadzu, Kyoto, Japan) and a TSK-GEL 80T_S column (4.6 mm \times 250 mm), and (A) 50 mM acetic acid-ammonium acetate and (B) acetonitrile were used as the eluents. A linear gradient of 90% A and 10% B changing over 60 min to 0% A and 100% B was used. The flow rate was controlled at 1.0 mL/min. After the eluate was obtained from the column, the three-dimensional data were processed with a diode array detector (SPD-M10A; Shimadzu).

Thioflavin-T measurement

Thioflavin-T measurement was performed using the method described by Suemoto *et al.* (2004) with slight modifications. For the A β aggregate-formation assay, A β (20 μ M) dissolved in the 50 mM potassium phosphate buffer (pH 7.4) with a test herbal extract was incubated at 37°C for 96 h (A β _{1–40}) or 24 h (A β _{1–42}). For the destabilization assay of pre-formed A β aggregates, after incubation of A β _{1–40} (96 h) or A β _{1–42} (24 h) without a test herbal extract, a mixture of the aggregated A β and a test herbal extract was incubated for 30 min at 37°C.

At the end of the incubation, 3 μ M thioflavin-T dissolved in 100 mM glycine buffer (pH 8.5) was added to the mixture. Fluorescence of thioflavin-T bound to A β aggregates was measured using a microplate reader (Spectramax GEMINI XS; Molecular Devices, Sunnyvale, CA, USA) (excitation at 442 nm and emission at 485 nm) after incubation for 30 min at 25°C. The percentage inhibition was calculated by comparing the fluorescence values of test samples with those of control solutions without herbal extracts.

Animals

Tg2576 APP^{sw} mice over-express a 695-amino acid splice form (Swedish mutation K670N M671I) of the human A β precursor protein (APP695) which resulted in a fivefold increase in A β _{1–40} and a 14-fold increase in A β _{1–42} with increasing age, driven by the hamster prion protein promoter. The animals were allowed free access to water and standard laboratory food in a facility with the temperature controlled at 24 \pm 1°C and relative humidity at 55 \pm 5%, with lights on from 7:00 to 19:00 hours daily. Behavioral studies were performed between 10:00 and 12:00 hours. Experimental protocols were approved by the Animal Care and Use Committee, Tohoku University Graduate School of Medicine, and complied with the procedures outlined in the Guide for the Care and Use of Laboratory Animals of Tohoku University.

Step-through passive-avoidance test

The apparatus (AP model; O'Hara Co., Tokyo, Japan) for the step-through passive-avoidance test consisted of two compartments, illuminated compartment [100 mm \times 120 mm \times 100 mm; light at the top of compartment (27W, 3000 lx)] and dark compartment (100 mm \times 170 mm \times 100 mm). The compartments were separated by a guillotine door. During the learning stage, a mouse was placed in the illuminated safe compartment. As the compartment was lit, the mouse stepped through the opened guillotine door into the dark compartment. The time spent in the illuminated compartment was defined as the latency time. Three seconds after the mouse entered the dark compartment, a foot shock (0.3 mA, 50V, 50 Hz ac, for 3 s) was delivered to the floor grids in the dark compartment. The mouse could escape from the shock only by stepping back to the safe illuminated compartment. Such acquisition trials during the learning stage were carried out once a day for 5 days. It was judged as learning avoidance from foot-shock if the mouse remained in the illuminated compartment for 300 s after being placed there. The retention trials were carried out once per week for 10 weeks from Days 8 to 78 to evaluate the retention of avoidance memory. The latency time was measured for up to 300 s without delivering foot-shock. It was judged that the mouse retained the avoidance memory when it stayed in the illuminated safe compartment for 300 s.

Acquisition and retention trials were conducted in 11-month-old mice.

Immunocytochemistry

All sample brains were fixed in neutral-buffered formalin and embedded in paraffin. Immunocytochemistry was performed using an Amyloid β Protein Immunohistochemical Kit (Wako Pure Chemical Industries, Ltd., Osaka, Japan) according to the manufacturer's instructions. Briefly, after deparaffinization, 8- μ m brain sections were immersed in 99% formic acid for 5 min, blocked with blocking serum, and immunostained with BA27 (A β _{1–40}) and BC05 (A β _{1–42}) by a standard avidin–biotin complex method, using 3,3'-diaminobenzidine as chromogen and lightly counter-staining with hematoxylin.

Tissue preparation

Tissue samples were processed in Tris-buffered saline (soluble fraction) and 70% formic acid (insoluble fraction) containing 1 \times protease inhibitor mixtures as described previously (Calon *et al.* 2004) with slight modifications. Briefly, brain tissues were homogenized and sonicated in Tris-buffered saline containing protease inhibitor mixture. The resulting homogenate was subjected to ultracentrifugation at 200 000 g at 4°C for 20 min, and the soluble supernatant was collected and frozen. To analyze the insoluble A β , the insoluble pellet was sonicated in 200 μ L of 70% formic acid and subjected to ultracentrifugation at 300 000 g at 4°C for 30 min, and the soluble supernatant was collected.

A β levels

Brain A β _{1–40} and A β _{1–42} levels were measured using sandwich ELISA with a Human β Amyloid ELISA Kit (Wako Pure Chemical Industries, Ltd.) according to the manufacturer's instructions. BAN50 is a monoclonal antibody raised against a synthetic peptide of human A β _{1–16}; it preferentially reacts with the N-terminal portion of human A β starting at Asp-1 but does not cross-react with N-terminally truncated A β nor with rodent-type A β . BA27 and BC05, which specifically recognize the C terminus of A β _{1–40} and A β _{1–42}, respectively, were conjugated with horseradish peroxidase and used as detector antibodies. Mice brain insoluble fractions described above were neutralized and subjected to BAN50/BA27 or BAN50/BC05 ELISA. The amount of A β was calculated by comparing these absorbance values with those of control solutions without herbal extract.

A β oligomerization analysis

Amount of A β _{1–42} oligomer was measured using A β Aggregate Human Singleplex Bead Kit (Invitrogen Corporation, Carlsbad, CA, USA) according to the manufacturer's instructions. Data analysis was performed by a flow cytometer (FACSCaliber, Becton Dickinson Immunocytometry Systems, Franklin Lakes, NJ, USA).

Cell viability assay

SK-N-SH cells were maintained in Dulbecco's modified Eagle's medium (Gibco Life Technologies, Carlsbad, CA, USA) supplemented with 10% fetal calf serum and 4 mM L-glutamine in a humidified atmosphere of 5% CO₂ and 95% air. SK-N-SH cells were seeded in 96-well plates at a density of 1 \times 10⁴ cells per well. After 24 h, we pre-incubated SK-N-SH cells for 30 min with PGG, followed by 24 h treatment with 10 μ M aggregated A β _{1–42}. Cell

viability was assessed using the 3-(4,5-dimethylthiazol-2-yl)-2,5-diphenyltetrazolium bromide (MTT) method. Absorbance values of formazan were determined at 590 nm with an automatic microplate reader.

Data analysis

Data were expressed as mean \pm SD. Statistical comparisons were made using ANOVA with Bonferroni's *post hoc* analysis. $p < 0.05$ was considered to be significant.

Results

Concentration-dependent effects of *Paeonia suffruticosa* on kinetics of A β fibril formation and breakdown

In our previous publication, it was noted that several medicinal herbs including *Uncaria rhynchophylla*, *Cinnamomum cassia*, and *Paeonia suffruticosa* showed destabilizing activity on A β fibrils (Fujiwara *et al.* 2006). *Paeonia suffruticosa* which was extracted either by water, methanol, or ethanol was concentrated under reduced pressure to yield oily residues (2.33, 1.89, and 2.14 g for water, methanol, and ethanol, respectively). To examine the inhibitory effect of *Paeonia suffruticosa* on A β fibril formation, concentration-dependencies were examined by the thioflavin T method. We

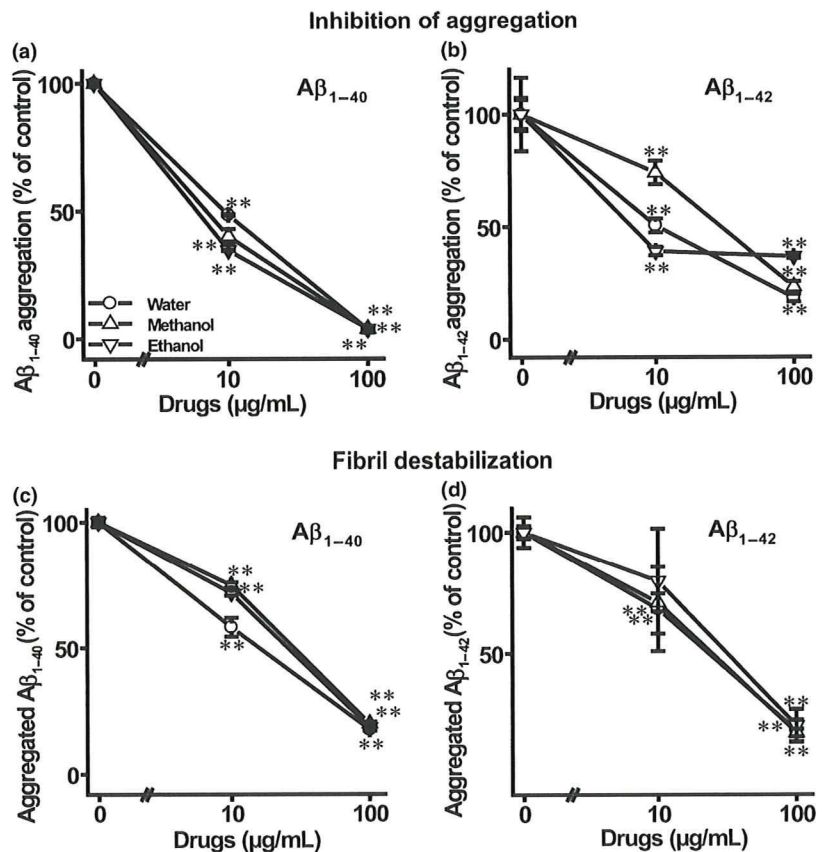
observed that fluorescence intensity in A β_{1-40} and A β_{1-42} declined in a concentration-dependent manner (Fig. 1a and b). A β_{1-40} fibril formation was inhibited by 10 μ g/mL of the water (48.5 \pm 0.3%), methanol (40.1 \pm 2.8%), and ethanol (34.6 \pm 0.2%) extracts of *Paeonia suffruticosa*. A β_{1-42} fibril formation was also inhibited by each of the three different extracts (10 μ g/mL), although the inhibitory concentration was lower than for A β_{1-40} .

In the analysis of fibril destabilization, fluorescence derived from thioflavin T was decreased in a dose-dependent manner after the addition of each of the extracts of *Paeonia suffruticosa* to pre-formed A β fibrils, and the degree of inhibition was similar to that observed on A β aggregation (Fig. 1c and d). Pre-formed A β_{1-40} fibrils were destabilized by 10 μ g/mL of the water (58.2 \pm 3.7%), methanol (74.9 \pm 1.1%) and ethanol (71.7 \pm 1.0%) extracts. Over 80% of pre-formed A β_{1-40} and A β_{1-42} fibrils were destabilized by each of the three different extracts at the concentration of 100 μ g/mL.

Step-through passive-avoidance tests

Step-through passive-avoidance tests were carried out in Tg2576 mice at 11 to 14 months of age. In the first acquisition trial of the learning stage, all mice (11 months

Fig. 1 Effects of three different *Paeonia suffruticosa* extracts on the kinetics of A β formation and destabilization. a and b: A β aggregate-formation assay. Reaction mixtures containing 20 μ M of A β_{1-40} (a) or A β_{1-42} , (b) 50 mM phosphate buffer (pH 7.4), and various extracts [water (circles), methanol (upward-pointing triangles), and ethanol (downward-pointing triangles)] were incubated at 37°C for 96 h (a) or 24 h (b). A β aggregation was expressed as percentage of the control sample which did not contain herbal extract. c and d: A β aggregate-destabilization assay. Reaction mixtures containing 20 μ M A β_{1-40} (c) or A β_{1-42} (d) were incubated at 37°C for 96 h (c) or 24 h (d). The extracts were then added and incubated for another 30 min. A β aggregation was assessed by the thioflavin T method and expressed as the percentage of control aggregation in the absence of herbal extract. Values represent mean \pm SD from four independent experiments. ** $p < 0.01$ compared with extract-untreated control.



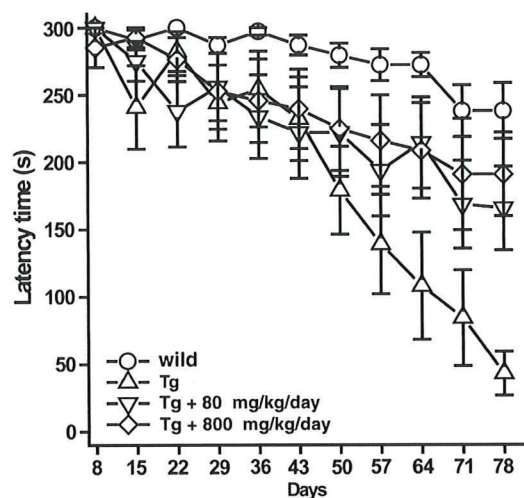


Fig. 2 Step-through latencies in the retention stages of the passive-avoidance task in *Paeonia suffruticosa*-treated transgenic (Tg2576) mice. Wild type and transgenic mice could acquire the avoidance memory by four or five repeated learning trials. The retention trials were carried out once per week for 10 weeks from Days 8 to 78 to evaluate the retention of avoidance memory. The latency time was measured for up to 300 s without delivering foot-shock. Wild type (Wild: circles); transgenic mice (Tg: upward-pointing triangles); 80 mg/kg/day *Paeonia suffruticosa* by repeated oral administration (Tg + 80 mg/kg/day: downward-pointing triangles), and 800 mg/kg/day *Paeonia suffruticosa* (Tg + 800 mg/kg/day: diamond). Values represent the means \pm SD from 11 to 17 independent experiments.

old) in the wild type and Tg groups entered the dark compartment immediately after being placed in the illuminated compartment. Repeating the acquisition trial increased the latency times in both groups. All mice in the wild type and Tg groups acquired avoidance memory, staying in the illuminated compartment for over 300 s on the fifth acquisition day. However, no significant differences were observed in the mean latency times between the wild type and Tg groups on any given day during the learning stage (data not shown). In retention trials (Fig. 2), the step-through latency of the Tg group was significantly reduced when compared with that of the wild type group. *Paeonia suffruticosa*-treated Tg mice were indistinguishable from non-transgenic littermates on days from 50 to 78 of testing.

A β pathology was reduced in *Paeonia suffruticosa*-treated Tg mice

To determine whether oral *Paeonia suffruticosa* treatment affected the accumulation of A β in brain tissue, we evaluated A β immunoreactivity in brain sections from untreated (Fig. 3a and c) and *Paeonia suffruticosa*-treated mice (Fig. 3b and d) using BA27 and BC05 antibodies which recognize the C-terminus of human A β ₁₋₄₀ (Fig. 3a and b)

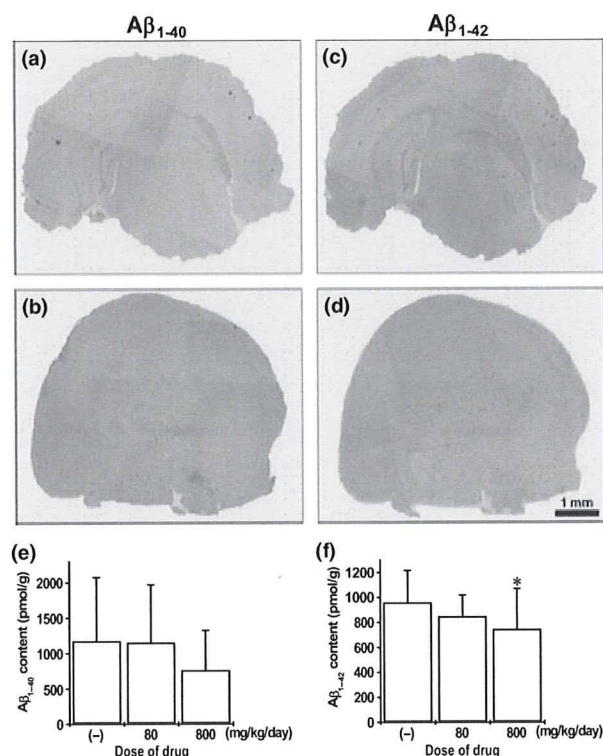


Fig. 3 Immunostaining (a–d) and ELISA analysis of formic acid-extractable A β levels (e and f) after dietary intake of *Paeonia suffruticosa* in Tg2576 mice. (a–d) Hemibrain cryostat sections were labeled with anti-A β ₁₋₄₀ (a and b) and A β ₁₋₄₂ (c and d) antibody. Image analysis was performed on the cerebral cortex from untreated (a and c) and *Paeonia suffruticosa*-treated (b and d) animals. Scale bar = 1 mm. Levels of A β ₁₋₄₀ (e) and A β ₁₋₄₂ (f) were quantified using an ELISA kit on formic acid-extractable A β from cortices of the low intake group (80 mg/kg/day) and high intake group (800 mg/kg/day). Values represent mean \pm SD from 11 to 17 independent experiments. * p < 0.05 compared with *Paeonia suffruticosa*-untreated control.

and A β ₁₋₄₂ (Fig. 3c and d). The number of A β -positive spots in the cortex and hippocampus were obviously lower in the *Paeonia suffruticosa*-treated mice compared with the untreated mice. No A β immunoreactivity was observed in brain sections from non-transgenic mice (data not shown).

We next measured the levels of A β ₁₋₄₀ and A β ₁₋₄₂ in brain tissue samples from Tg mice using a sensitive ELISA method (Fig. 3e and f). Consistent with the results of A β immunostaining, the A β ₁₋₄₂ concentration in the samples from *Paeonia suffruticosa*-treated Tg mice (800 mg/kg/day) was significantly lower than the concentration in *Paeonia suffruticosa*-untreated mice ($747.8 \pm 322.4\%$, $p < 0.05$). In contrast to its effect on A β ₁₋₄₂ levels, *Paeonia suffruticosa* treatment had no significant effect on A β ₁₋₄₀ levels in the Tg mice. The levels of A β ₁₋₄₀ and A β ₁₋₄₂ were below the limit of detection in cerebral cortex samples from non-transgenic mice (data not shown).

HPLC analyses of *Paeonia suffruticosa*: identification of four different natural compounds and their effects on the kinetics of A β_{1-42} formation and destabilization

The three-dimensional-HPLC fingerprints of water extracts of *Paeonia suffruticosa* are illustrated in Fig. 4. The water extract contained several different chemical compounds including paeonol, benzoic acid, and derivatives of paeoniflorin as well as PGG.

Concentration dependence of the inhibitory effects of these compounds on A β fibril formation was examined using the thioflavin T method (Fig. 5a). Only PGG induced a concentration-dependent decline in the thioflavin T fluorescence intensity associated with A β_{1-42} . PGG (3 μ M) inhibited A β_{1-42} fibril formation by more than 50%. Additional thioflavin-T experiments were performed in order to determine the ability of PGG to destabilize pre-formed A β fibrils. Fluorescence derived from thioflavin T was decreased in a dose-dependent manner after the addition of PGG to pre-formed A β fibrils to an extent similar to that seen for the inhibition of A β aggregation (Fig. 5b).

Next, we incubated different concentrations of PGG with unpolymerized A β_{1-42} (10 μ M) and monitored the formation of amyloid using the Thioflavin T method (Fig. 6). In the absence of PGG, A β_{1-42} formed Thioflavin T-binding aggregates after a lag phase of 2 h, whereas thioflavin T signals were decreased to 33.6 \pm 16.8% by 1 μ M PGG after

a lag phase of 24 h. Moreover, A β_{1-42} aggregation was completely inhibited by 100 μ M PGG.

Effect of PGG on A β_{1-42} oligomers

To further characterize the breakdown products that accumulated in the presence of PGG, aliquots of A β_{1-42} oligomerization reaction mixtures in the presence or absence of PGG were assayed by flow cytometric analysis (Fig. 7). In the absence of PGG, the fluorescence intensity of A β_{1-42} oligomerized sample was potent compared with vehicle sample without A β_{1-42} oligomers (Fig. 7a and b). Samples treated with PGG reduced the fluorescence intensity in a concentration-dependent manner (Fig. 7c–e). These data confirmed that PGG was a strong inhibitor of A β_{1-42} oligomerization.

Neuroprotective effects of PGG against A β toxicity

To evaluate whether PGG could potentially prevent A β -induced toxicity, we pre-incubated SK-N-SH cells for 30 min with PGG, followed by 24 h treatment with 10 μ M aggregated A β_{1-42} . SK-N-SH cell viability was significantly impaired by A β peptides, measured by MTT assay. PGG (10 μ M) significantly protected SK-N-SH cells against A β -induced toxicity. When measured by MTT reduction, cell survival was restored from 56.9 \pm 2.5% to 87.0 \pm 13.6% in response to the A β_{1-42} aggregates (Fig. 8).

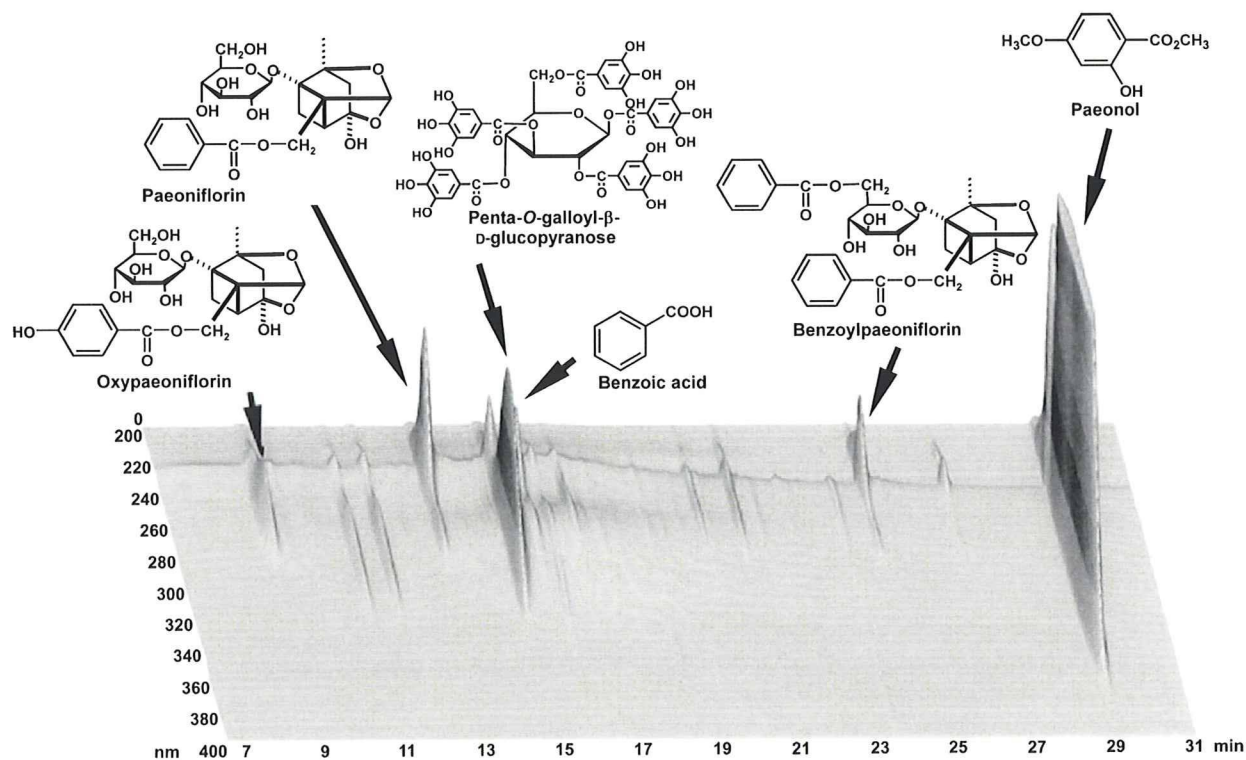


Fig. 4 Identification of chemicals by three-dimensional HPLC analysis of the water extract of *Paeonia suffruticosa*. Each peak indicates a molecule described in the figure.

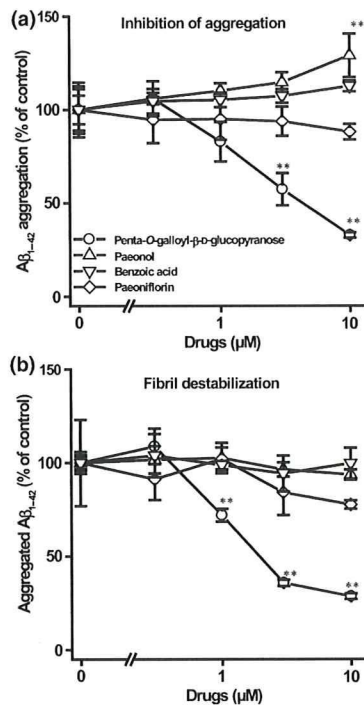


Fig. 5 Effects of distinct compounds isolated from *Paeonia suffruticosa* on the kinetics of A β s formation and destabilization. a: A β aggregate-formation assay. Reaction mixtures containing 20 μ M of A β_{1-42} , 50 mM phosphate buffer (pH 7.4), and various compounds [1,2,3,4,6-penta-O-galloyl- β -D-glucopyranose (circles), paeonol (upward-pointing triangles), benzoic acid (downward-pointing triangles), and paeoniflorin (diamond)] were incubated at 37°C for 24 h. A β aggregation is expressed as percentage of control observed in the absence of test compounds. b: A β aggregate-destabilization assay. Reaction mixtures containing 20 μ M A β_{1-42} were incubated at 37°C for 24 h. The extracts were added and incubated for 30 min. A β aggregation was assessed by the thioflavin T method and expressed as percentage of control aggregation observed in the absence of test compounds. Values represent mean \pm SD from four independent experiments. ** $p < 0.01$ compared with extract-untreated control.

A β pathology is diminished in PGG-treated Tg mice

To determine the effect of oral PGG treatment accumulation of A β in Tg type mice, we evaluated A β immunoreactivity in brain sections from untreated and PGG-treated mice by using antibodies BA27 and BC05 (Fig. 9a–d). The number of A β -positive spots in the hippocampus was obviously lower in PGG-treated mice (Fig. 9b and d) compared with untreated mice (Fig. 9a and c). No A β immunoreactivity was observed in brain sections from non-transgenic mice (data not shown).

We next measured the levels of A β_{1-40} and A β_{1-42} in brain samples from Tg mice by using a sensitive ELISA method (Fig. 9e and f). In the brains of Tg mice treated with PGG by repeated oral administration, the A β_{1-40} and A β_{1-42} concentrations were significantly lower (2417.5 \pm 279.5% and

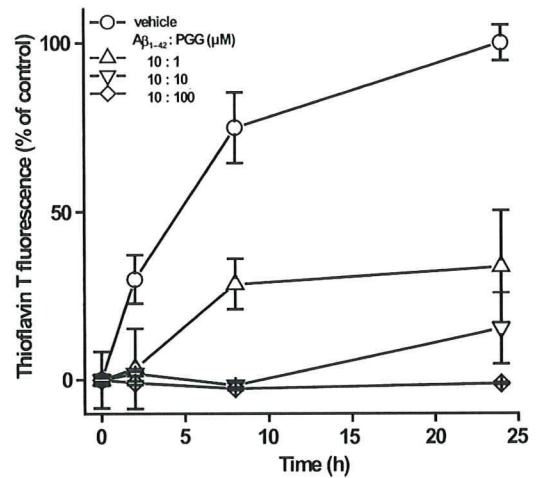


Fig. 6 The molar ratio of the A β -PGG interaction. Reaction mixtures containing 10 μ M A β_{1-42} : PGG [solvent alone (circles), molar ratio 10 : 1 (upward-pointing triangles), 10 : 10 (downward-pointing triangles), and 10 : 100 (diamond)] were incubated at 37°C for indicated time. Thioflavin T fluorescence was expressed as a percentage of control which was observed at the point of 24 h without PGG. Values represent mean \pm SD from four independent experiments.

46.8 \pm 3.0%, $p < 0.01$) than those in PGG-untreated mice. The levels of A β_{1-40} and A β_{1-42} were below the limit of detection in cerebral cortex samples from non-transgenic mice (data not shown).

Discussion

In AD research, much attention has focused on altering the course of the disease through early diagnosis and intervention. Clinical application of biomarkers and amyloid imaging may be attractive and realistic diagnostic procedures by which to identify the disease early. On the other hand, safety is an important concern with regard to early intervention with disease modifying drugs. *Paeonia suffruticosa* has been used medicinally in humans for more than 1000 years with virtually no toxic effects reported.

The results of our studies using thioflavin T fluorescence demonstrated that *Paeonia suffruticosa* extracts, regardless of the extraction method used, could inhibit the assembly of A β fibrils. All three extracts (water, methanol, and ethanol) induced a dramatic decline in the fluorescence intensity of thioflavin T in the μ g/mL range. In our preliminary experiment, we confirmed that these extracts did not quench thioflavin T fluorescence at the indicated concentrations. These results suggest two possibilities; one is that *Paeonia suffruticosa* indeed destabilizes A β fibrils, and the other is that it antagonizes the binding of thioflavin T to A β . It has been reported that absorbance of Congo red was increased by binding to A β protein as well as to thioflavin T. The binding site in A β to Congo red was different from that to thioflavin

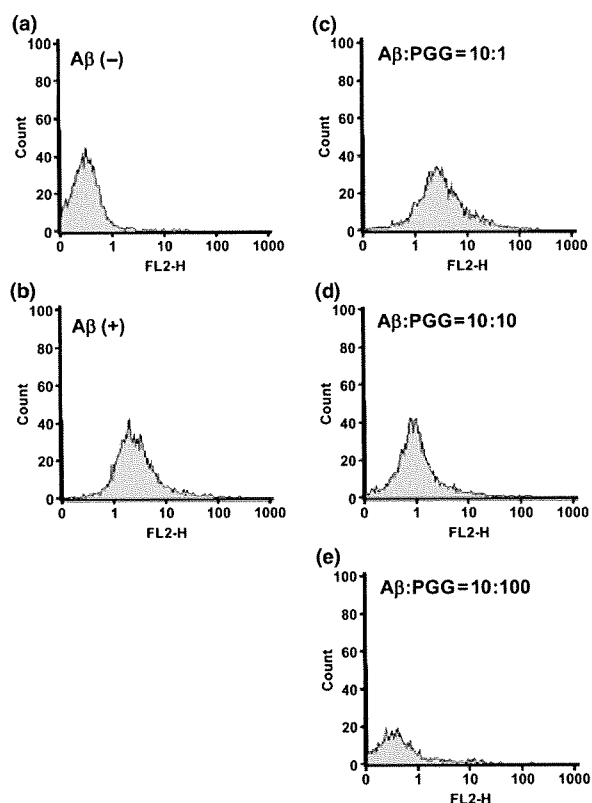


Fig. 7 Effects of PGG on A β ₁₋₄₂ oligomeric species. These histograms were developed using reagents provided in the Aggregated A β Assay Kit. a: buffer-control; b: 10 μ M A β ₁₋₄₂ in absent of PGG; c-e: 10 μ M A β ₁₋₄₂ with PGG molar ratio 10 : 1 (c), 10 : 10 (d), and 10 : 100 (e).

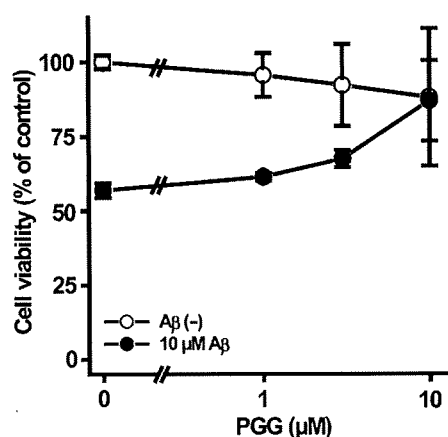


Fig. 8 Effects of PGG against A β -induced toxicity. SK-N-SH cells were pre-treated without or with PGG for 30 min followed by incubation without or with A β ₁₋₄₂ (10 μ M) for 24 h. Cell viability was assessed by MTT method and expressed as a percentage of control viability, which was observed in the absence of A β ₁₋₄₂ and PGG. Values represent the means \pm SD from four independent experiments.

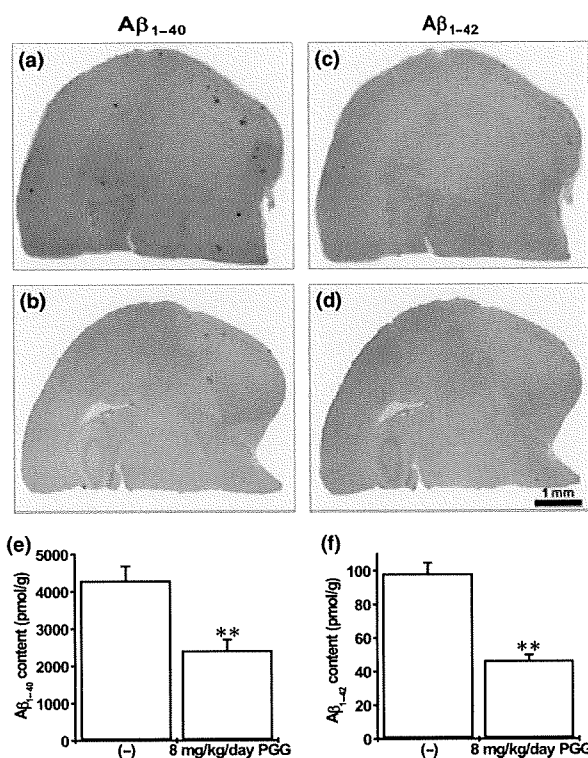


Fig. 9 Immunostaining (a-d) and ELISA analysis of formic acid-extractable A β levels (e and f) after dietary intake of 1,2,3,4,6-penta-*O*-galloyl- β -*D*-glucopyranose (PGG) in Tg2576 mice. (a-d) Hemibrain cryostat sections were labeled with anti-A β ₁₋₄₀ (a and b) and A β ₁₋₄₂ (c and d) antibody. Image analysis was performed on the cerebral cortices from PGG-untreated (a and c) and -treated (b and d) animals. Scale bar = 1 mm. Levels of A β ₁₋₄₀ (e) and A β ₁₋₄₂ (f) were quantified on formic acid-extractable A β from cortices of the 8 mg/kg/day PGG groups. Values represent mean \pm SD from seven to eight independent experiments. ***p* < 0.01, compared with PGG-untreated control.

T. In our experiments, each of the three *Paeonia suffruticosa* extracts decreased the absorbance of Congo red (data not shown), suggesting that the decrease in thioflavin T fluorescence by *Paeonia suffruticosa* extracts was caused by destabilization of A β fibrils. Moreover, our preliminary atomic force microscopy data also strongly support this notion, as destabilization of A β fibrils by *Paeonia suffruticosa* extracts was directly visualized (data not shown). The extracts of *Paeonia suffruticosa* inhibited aggregation of both A β ₁₋₄₀ and A β ₁₋₄₂ to a similar extent. Therefore, the inhibitory effect of *Paeonia suffruticosa* on amyloidogenesis of A β may not be dependent on the distinct amino acid sequence of its C-terminal.

Paeonia suffruticosa treatment prevented A β -related memory deficits and AD-type neuropathology *in vivo*. In our study, we found that treatment of Tg2576 mice with *Paeonia suffruticosa* attenuated memory deterioration, and this effect coincided with an approximately 20% reduction in

A β peptide content in the brain. We hypothesize that treatment with *Paeonia suffruticosa* may have beneficial effects on AD-type memory deterioration through a direct interaction between *Paeonia suffruticosa* and A β peptides in the brain, leading to the prevention of A β plaque formation.

Our studies also showed that PGG at low concentrations (IC₅₀ = 3 μ M) can inhibit A β aggregation or promote its destabilization. Moreover, our preliminary scanning electron microscopy data also strongly support this notion, as destabilization of A β fibrils by PGG was directly visualized (Fig. S1). As other chemical compounds, such as paeonol, benzoic acid, and paeoniflorin had no effects on A β aggregation, PGG may be the principal active constituent responsible for the effect of *Paeonia suffruticosa* on A β fibril regulation. Previous published literatures reported that several polyphenols, such as those from green tea or grape, had anti-aggregation property (Ehrnhoefer *et al.* 2008; Rivière *et al.* 2008). PGG had a comparable inhibitory effect with such published polyphenols.

The toxicity of A β is becoming more strongly linked to the formation of oligomeric aggregates (Kirkitadze *et al.* 2002). In our experiments, PGG inhibited A β oligomerization. Moreover, treatment of SK-N-SH cells with PGG significantly protected the cells from A β ₁₋₄₂ toxicity at concentrations similar to those that inhibited A β aggregation. Thus, our experiments suggest that PGG inhibited not only A β fibril formation but also neurotoxic A β oligomer formation. Furthermore, oral intake of PGG reduced A β plaque burden and A β peptide content in brain tissue from Tg2576 mice, as did like *Paeonia suffruticosa*. There are two possible explanations; one is that PGG indeed destabilizes A β fibrils, and the other is that it inhibits the A β production or its secretion in Tg2576 mice brain. We demonstrated that PGG did not affect the level of full-length APP in Tg2576 mice (Figure S2), suggesting that the decrease in A β plaques and A β peptide content in brain tissue from Tg2576 mice by PGG may be caused by destabilization of A β fibrils. Curcumin, an active compound of *Curcuma longa*, was reported to inhibit A β fibril formation and to destabilize pre-formed A β fibrils *in vitro* and *in vivo* (Ono *et al.* 2004; Yang *et al.* 2005). It has also been reported that this compound is highly hydrophobic and should readily enter the brain to bind to plaques *in vivo* (Yang *et al.* 2005). Although highly hydrophilic, unlike curcumin, PGG has curcumin-like activity on A β fibril regulation *in vivo*. Studies of the metabolism of PGG and its ability to penetrate the blood-brain barrier by this compound are now underway.

In conclusion, our study demonstrates that *Paeonia suffruticosa* and PGG not only inhibit A β fibril formation but also disassemble pre-formed A β fibrils. Moreover, our experiments suggest that PGG inhibits A β oligomerization and A β toxicity. As a result, it improved memory deficits in Tg2576 mice. Therefore, extracts of *Paeonia suffruticosa* and PGG could have potential as therapeutic drugs for AD

patients and may also be useful as primary or secondary preventive agents for healthy individuals and patients with mild cognitive impairment. Furthermore, *Paeonia suffruticosa* has a satisfactory safety profile because no obvious adverse effects of *Pilulae octo-medicamentorum rehmanniae* have been reported. In our preliminary experiments, *Paeonia suffruticosa* was tested for hepatotoxicity, nephrotoxicity, and other biochemical parameters in transgenic mice. Fortunately, this medicinal herb did not show any signs of organ toxicity. Thus, *Paeonia suffruticosa* appears to be a safe natural product for regulating A β aggregation. *Paeonia suffruticosa* and PGG may represent a new class of therapeutic and preventive agents for AD which act to regulate the formation and the clearance of senile plaques.

Acknowledgements

This work was partially supported by (i) a grant-in-aid for scientific research from the Ministry of Education, Science, Sports and Culture of Japan (#16590554), (ii) a program for the promotion of fundamental studies in Health Science of the National Institute of Biomedical Innovation (NIBIO) of Japan (#03-1), and (iii) a grant-in-aid from Core Research for Evolutional Science and Technology of Japan Science and Technology Corporation. We thank S. Isogami and M. Takahashi for kind advice and technical supports.

Supporting Information

Additional Supporting Information may be found in the online version of this article:

Figure S1 Scanning electron microscope imaging of A β ₁₋₄₂ fibrils. After incubation of A β ₁₋₄₂ for 24 h for preformed fibrils, the mixture of aggregated A β and the PGG was incubated at 37°C for 1 h. A: vehicle (DMSO); B: 10 μ M A β ₁₋₄₂; 10 μ M PGG (molar ratio 1 : 1). Scale bar = 5 μ m.

Figure S2 Effects of PGG on the level of amyloid precursor protein (APP) in Tg2576 mice. Immunoblotting of brain levels of APP after dietary 1,2,3,4,6-penta-*O*-galloyl- β -D-glucopyranose (PGG) in Tg2576. Levels of APP were quantitated by immunoblotting with full length APP antibody from cortices of 8 mg/kg/day-PGG groups. The samples were separated on a 10% polyacrylamide gel, followed by immunoblotting with anti-full length APP antibody. Arrowheads point to APP. Similar results were obtained from at least 3 independent experiments.

Please note: Wiley-Blackwell are not responsible for the content or functionality of any supporting materials supplied by the authors. Any queries (other than missing material) should be directed to the corresponding author for the article.

References

- Anderton B. H., Callahan L., Coleman P. *et al.* (1998) Dendritic changes in Alzheimer's disease and factors that may underlie these changes. *Prog. Neurobiol.* **55**, 595–609.
- Barghorn S., Nimmrich V., Striebinger A. *et al.* (2005) Globular amyloid beta-peptide oligomer – a homogenous and stable neuropathological protein in Alzheimer's disease. *J. Neurochem.* **95**, 834–847.

- Barrow C. J. and Zagorski M. G. (1991) Solution Structures of β -peptide and its constituent fragments: relation to amyloid deposition. *Science* **253**, 179–182.
- Calon F., Lim G. P., Yang F. *et al.* (2004) Docosahexaenoic acid protects from dendritic pathology in an Alzheimer's disease mouse model. *Neuron* **43**, 633–645.
- Chou T. C. (2003) Anti-inflammatory and analgesic effects of Paeonol in carrageenan-evoked thermal hyperalgesia. *Br. J. Pharmacol.* **139**, 1146–1152.
- Darreh-Shori T., Hellstrom-Lindahl E., Flores-Flores C. *et al.* (2004) Long-lasting acetylcholinesterase splice variations in anticholinesterase-treated Alzheimer's disease patients. *J. Neurochem.* **88**, 1102–1113.
- Ehrnhoefer D. E., Bieschke J., Boeddrich A. *et al.* (2008) EGCG redirects amyloidogenic polypeptides into unstructured, off-pathway oligomers. *Nat. Struct. Mol. Biol.* **15**, 558–566.
- Fujiwara H., Iwasaki K., Furukawa K. *et al.* (2006) *Uncaria rhynchophylla*, a Chinese medicinal herb, has potent antiaggregation effects on Alzheimer's beta-amyloid proteins. *J. Neurosci. Res.* **84**, 427–433.
- Hofmann T., Glabasnia A., Schwarz B. *et al.* (2006) Protein binding and astringent taste of a polymeric procyanidin, 1,2,3,4,6-penta-O-galloyl-beta-D-glucopyranose, castalagin, and grandinin. *J. Agric. Food. Chem.* **54**, 9503–9509.
- Hsieh C. L., Cheng C. Y. and Tsai T. H. (2006) Paeonol reduced cerebral infarction involving the superoxide anion and microglia activation in ischemia-reperfusion injured rats. *J. Ethnopharmacol.* **106**, 208–215.
- Iwasaki K., Kobayashi S., Chimura Y. *et al.* (2004) A randomized, double-blind, placebo-controlled clinical trial of the Chinese medicinal herb "ba wei di huang wan" in the treatment of dementia. *J. Am. Geriatr. Soc.* **52**, 1518–1521.
- Iwasaki K., Satoh-Nakagawa T., Maruyama M. *et al.* (2005) A randomized, observer-blind, controlled trial of the traditional Chinese medicine Yi-Gan San for improvement of behavioral and psychological symptoms and activities of daily living in dementia patients. *J. Clin. Psychiatry* **66**, 248–252.
- Kirkitadze M. D., Bitan G. and Teplow D. B. (2002) Paradigm shifts in Alzheimer's disease and other neurodegenerative disorders: the emerging role of oligomeric assemblies. *J. Neurosci. Res.* **69**, 567–577.
- Le Bars P. L., Katz M. M., Berman N. *et al.* (1997) A placebo-controlled, double-blind, randomized trial of an extract of Ginkgo biloba for dementia. North American EGb Study Group. *JAMA* **278**, 1327–1332.
- Li Y., Kim J., Li J. *et al.* (2005) Natural anti-diabetic compound 1,2,3,4,6-penta-O-galloyl-D-glucopyranose binds to insulin receptor and activates insulin-mediated glucose transport signaling pathway. *Biochem. Biophys. Res. Commun.* **336**, 430–437.
- Lin H. C., Ding H. Y., Ko F. N. *et al.* (1999) Aggregation inhibitory activity of minor acetophenones from *Paeonia* species. *Planta Med.* **65**, 595–599.
- Millard C. B. and Broomfield C. A. (1995) Anticholinesterases: medical applications of neurochemical principles. *J. Neurochem.* **64**, 1909–1918.
- Nakagawasai O., Yamadera F., Iwasaki K. *et al.* (2004) Effect of kami-untan-to on the impairment of learning and memory induced by thiamine-deficient feeding in mice. *Neuroscience* **125**, 233–241.
- Ono K., Hasegawa K., Naiki H. *et al.* (2004) Curcumin has potent anti-amyloidogenic effects for Alzheimer's beta-amyloid fibrils in vitro. *J. Neurosci. Res.* **75**, 742–750.
- Park C. H., Lee Y. J., Lee S. H. *et al.* (2000) Dehydroevodiamine HCl prevents impairment of learning and memory and neuronal loss in rat models of cognitive disturbance. *J. Neurochem.* **74**, 244–253.
- Rivière C., Richard T., Vitrac X. *et al.* (2008) New polyphenols active on beta-amyloid aggregation. *Bioorg. Med. Chem. Lett.* **18**, 828–831.
- Selkoe D. J. (2002) Alzheimer's disease is a synaptic failure. *Science* **298**, 789–791.
- Suemoto T., Okamura N., Shiomitsu T. *et al.* (2004) *In vivo* labeling of amyloid with BF-108. *Neurosci. Res.* **48**, 65–74.
- Suzuki T., Arai H., Iwasaki K. *et al.* (2001) A Japanese herbal medicine (Kami-Untan-To) in the treatment of Alzheimer's disease: A pilot study. *Alzheimer's Rep.* **4**, 177–182.
- Tierney M. C., Fisher R. H., Lewis A. J. *et al.* (1988) The NINCDS-ADRDA Work Group criteria for the clinical diagnosis of probable Alzheimer's disease: a clinicopathologic study of 57 cases. *Neurology* **38**, 346–359.
- Wirhth O., Multhaup G. and Bayer T. A. (2004) A modified β -amyloid hypothesis: intraneuronal accumulation of the β -amyloid peptide – the first step of a fatal cascade. *J. Neurochem.* **91**, 513–520.
- Yang F., Lim G. P., Begum A. N. *et al.* (2005) Curcumin inhibits formation of amyloid beta oligomers and fibrils, binds plaques, and reduces amyloid in vivo. *J. Biol. Chem.* **280**, 5892–5901.
- Yasuda T., Kon R., Nakazawa T. *et al.* (1999) Metabolism of Paeonol in rats. *J. Nat. Prod.* **62**, 1142–1144.

Expert Opinion

1. Introduction
2. Cerebral glucose metabolism and cerebral blood flow
3. Imaging neurotransmitter, neuroreceptor and neuroenzymatic function
4. Imaging of neuroinflammation
5. Imaging amyloid deposits in the brain
6. Expert opinion

Advances in molecular imaging for the diagnosis of dementia

Nobuyuki Okamura, Michelle T Fodero-Tavoletti, Yukitsuka Kudo, Christopher C Rowe, Shozo Furumoto, Hiroyuki Arai, Colin L Masters, Kazuhiko Yanai & Victor L Villemagne[†]

[†]Center for PET, Austin Health, Nuclear Medicine, Melbourne, Australia

Background: There is an urgent need for early diagnosis and treatment of dementia to ease caregiver burden and medical costs associated with the increasing number of affected patients. Molecular imaging with target-specific ligands is contributing to the early diagnosis of dementia and the evaluation of anti-dementia therapy. **Objective:** This article reviews recent advances in the molecular imaging field applied to dementia. To illustrate the utility of molecular imaging in the clinical management of dementia, results from recently published papers using new imaging probes are compared with those from conventional imaging strategies. **Conclusion:** The recent development of β -sheet binding agents including FDDNP, PIB, SB-13, BF-227 and BAY94-9172 enables the non-invasive detection of amyloid deposition in the brain. These agents would be useful for the early and accurate diagnosis of Alzheimer's disease, patient selection for disease-modifying therapeutic trials and monitoring the effect of anti-amyloid therapy. Also, monitoring neurotransmitter function contributes to the differential diagnosis of dementia and refinement of treatment protocols. New targets for molecular imaging are focusing on protein misfolding diseases associated with the neurotoxic deposition of aggregated tau, α -synuclein and prion proteins.

Keywords: acetylcholine, Alzheimer's disease, amyloid- β protein, dementia, imaging, molecular imaging, near-infrared, positron emission tomography, prion, single photon emission computed tomography, tau

Expert Opin. Med. Diagn. (2009) 3(6):705-716

1. Introduction

Dementia is a common and life-threatening disease in elderly people. The prevalence of dementia increases after the age of 65, resulting in an increasing medical and socio-economic burden. Alzheimer's disease (AD) is the most common cause of dementia and currently affects 4 million people in the US. AD generally begins insidiously with mild memory problems and progresses to the development of functional impairment in multiple cognitive domains within a few years. Elderly people usually complain of increasing forgetfulness with age. However, not all subjects with mild memory impairments progress to dementia. It is important to develop diagnostic methods that have adequate sensitivity and specificity to distinguish those who are likely to develop AD from those memory-impaired individuals who do not. In addition, it is important to predict accurately who might be at an increased risk for AD from a large pool of elderly people. The arrival of new therapies that may delay disease progression emphasizes the need to improve the diagnostic certainty early in the course of AD.

Structural neuroimaging techniques, such as computed tomography (CT) and magnetic resonance imaging (MRI), are routinely used in the screening of cerebrovascular and space-occupying lesions, in the differential diagnosis of normal-pressure hydrocephalus and AD, and in the evaluation of brain atrophy. Widespread cortical

informa
healthcare

atrophy, a thinning of the medial temporal lobe structures and white matter hyperintensities are, although not pathognomonic, consistent structural neuroimaging findings associated with the progression of AD, where there is a significant overlap with the normal ageing process and with other pathological conditions. Modern molecular neuroimaging techniques such as positron emission tomography (PET) and single photon emission computed tomography (SPECT) have helped in the differential diagnosis of dementia while also allowing the exploration of specific molecular mechanisms of AD.

The pathological hallmarks of AD are the deposition of senile plaques (SPs) and neurofibrillary tangles (NFTs). Whereas NFTs are intraneuronal bundles of paired helical filaments mainly composed of the aggregates of an abnormally phosphorylated form of tau protein, senile plaques consist of extracellular aggregates of amyloid β -peptide ($A\beta$). Dementia with Lewy bodies (DLB) represents the second most frequent cause of neurodegenerative dementia in the elderly. Insoluble aggregates of α -synuclein called Lewy bodies are the pathological hallmarks of DLB as well as Parkinson's disease (PD), however Lewy bodies are found not only in PD and DLB, but also in AD and other neurodegenerative conditions. Furthermore, neocortical $A\beta$ burden is frequently observed in DLB patients, indicating substantial overlap in the pathology of AD and DLB. To understand precisely the molecular mechanisms of dementia, it is thus important to identify the contribution of each of these pathologies to the dementia syndrome.

2. Cerebral glucose metabolism and cerebral blood flow

Molecular neuroimaging using PET and SPECT has been widely used for the early and differential diagnosis of dementia. Regional hypoperfusion and hypometabolism in the posterior cingulate and temporoparietal cortices is one of the earliest changes in AD and is a prognostic marker in subjects with mild cognitive impairment (MCI) [1]. The development of voxel-by-voxel analysis techniques has made substantial contributions to the early identification of these regional brain changes [2]. A comparison study of fluoro-deoxy glucose (FDG)-PET and perfusion SPECT indicated that FDG-PET is more sensitive than SPECT because the magnitude of the hypometabolism observed with FDG-PET is generally greater than the degree of the hypoperfusion seen with SPECT [3]. FDG-PET is a sensitive technique for the early identification of AD patients where hypometabolism has been observed even in cognitively normal individuals who have a higher genetic risk of developing AD [4]. In a multi-center study, the prognostic value of FDG-PET showed a high degree of sensitivity (93%) in the evaluation of dementia [5]. However, the specificity (73%) is not completely at a satisfactory level for the prediction of progressive dementia.

Another important application of FDG-PET lies in the differential diagnosis of AD from other causes of dementia,

such as DLB and frontotemporal dementia (FTD). The consortium on dementia with Lewy bodies (CDLB) characterized DLB as a progressive cognitive decline, extrapyramidal symptoms, episodic confusion, hallucinations and fluctuating cognitive impairment [6]. However, several follow-up studies indicated that although the CDLB criteria present an appropriate specificity, it is laden with a relatively poor sensitivity [7]. In addition, differential diagnosis of DLB from AD is difficult even in the later stages of the disease. DLB differs from AD in the treatment response experienced by patients. For example, DLB patients are at high risk for severe reactions to antipsychotic drugs. This highlights a need to develop a sensitive diagnostic tool to provide greater precision in the ante-mortem diagnosis of DLB. Clinical PET and SPECT studies showed a characteristic pattern of regional glucose hypometabolism and hypoperfusion in the primary visual cortex and the occipital association cortex in addition to the temporoparietal pattern of abnormal cerebral blood flow and metabolism found in AD [8].

The ideal biomarker for AD should have a diagnostic sensitivity > 80% for detecting AD and a specificity of > 80% for distinguishing other dementias. Hanyu *et al.* indicated that a diagnostic strategy combining perfusion SPECT and mini mental state examination (MMSE) performance has produced a sensitivity of 81% and a specificity of 85% in the differentiation of DLB from AD [9], which indicates that perfusion SPECT is an ideal diagnostic marker for DLB. PET measures of glucose hypometabolism and SPECT measures of hypoperfusion in the occipital cortex could help to enhance the clinical diagnosis of DLB, particularly in the early stages of the disease, allowing the maximum therapeutic benefit in the treatment of DLB patients. A recent multi-center study demonstrated the usefulness of FDG-PET in the differential diagnosis of AD, DLB and FTD [10]. Differential diagnosis of AD and FTD is a particularly good application for FDG-PET because of the sharp contrast in their pattern of glucose hypometabolism. The addition of FDG-PET to clinical information increased the diagnostic accuracy and confidence for both AD and FTD [11]. In the US, the Center for Medicare and Medicaid Services has recently approved the use of FDG-PET for differential diagnosis of AD from FTD.

3. Imaging neurotransmitter, neuroreceptor and neuroenzymatic function

The evaluation of neurotransmitter functions in the brain is helpful for the determination and monitoring of treatment protocols, prediction of disease progression, as well as for the early diagnosis of dementia. Many radiotracers have been developed for the assessment of neurotransmitter functions, including dopamine, acetylcholine (ACh), serotonin, histamine, benzodiazepine, adenosine, NK-1 and opioid (Table 1) [12]. Some of them have been applied for the assessment of the neurotransmitter changes in dementia [13,14].

Table 1. Radiopharmaceuticals for brain positron emission tomography imaging.

Functions	Drugs
Blood flow	$^{15}\text{O-H}_2\text{O}$
Blood volume	$^{15}\text{O-CO}$
Glucose metabolism	$^{18}\text{F-FDG}$
Oxygen metabolism	$^{15}\text{O-O}_2$
Hypoxia	$^{18}\text{F-fluoromisonidazole}$
Amino acid metabolism	$^{11}\text{C-methionine}$
<i>Neurotransmitter</i>	
Dopamine D ₁ receptor	$^{11}\text{C-SCH23390}$, $^{11}\text{C-NNC112}$
Dopamine D ₂ receptor	$^{11}\text{C-raclopride}$, $^{11}\text{C-methylspiperone}$, $^{11}\text{C-nemonapride}$, $^{11}\text{C-FLB457}$
Dopamine transporter	$^{11}\text{C-}\beta\text{-CIT}$, $^{11}\text{C-CFT}$, $^{11}\text{C-cocaine}$, $^{11}\text{C-methylphenidate}$, $^{11}\text{C-PE2I}$
Dopamine synthesis	$^{11}\text{C-DOPA}$, $^{18}\text{F-DOPA}$
Muscarinic acetylcholine receptor	$^{11}\text{C-NMPB}$, $^{11}\text{C-TRB}$, $^{18}\text{F-FP-TZTP}$
Nicotinic acetylcholine receptor	$^{11}\text{C-nicotine}$, $^{18}\text{F-norchloro-fluoro-homoepibatidine}$, $^{18}\text{F-fluoro-A-85380}$
Acetylcholine esterase	$^{11}\text{C-MP4A}$, $^{11}\text{C-PMP}$, $^{11}\text{C-physostigmine}$, $^{11}\text{C-donepezil}$
Serotonin 5-HT _{1A} receptor	$^{11}\text{C-WAY100635}$, $^{18}\text{F-FCWAY}$
Serotonin 5-HT _{2A} receptor	$^{11}\text{C-methylspiperone}$, $^{11}\text{C-MDL 100907}$, $^{18}\text{F-altenserin}$, $^{18}\text{F-setoperone}$
Histamine H ₁ receptor	$^{11}\text{C-doxepin}$, $^{11}\text{C-pyramilamine}$
Central benzodiazepine receptor	$^{11}\text{C-flumazenil}$, $^{18}\text{F-flumazenil}$
Peripheral benzodiazepine receptor	$^{11}\text{C-PK11195}$, $^{11}\text{C-FEDAA1106}$, $^{11}\text{C-PBR28}$, $^{11}\text{C-DPA-713}$, $^{11}\text{C-CLINME}$
Adenosine receptor	$^{11}\text{C-MPDX}$, $^{11}\text{C-TMSX}$
NK-1 receptor	$^{11}\text{C-CP-99994}$, $^{18}\text{F-SPA-RQ}$
Opioid receptor	$^{11}\text{C-carfentanyl}$, $^{11}\text{C-diprenorphine}$, $^{18}\text{F-cyclofoxy}$
<i>Protein aggregate</i>	
Amyloid β protein	$^{11}\text{C-PIB}$, $^{11}\text{C-SB13}$, $^{11}\text{C-BF227}$, $^{18}\text{F-FDDNP}$, $^{18}\text{F-BAY94-9172}$

One of the major alterations found in the brains of AD patients is a loss of neurons in the cholinergic nucleus basalis of Meynert [15]. A loss of the cholinergic markers cholineacetyltransferase (ChAT) and acetylcholinesterase (AChE) is observed in post-mortem AD brains [16]. In addition, a loss of the cholinergic function is closely related with the severity of cognitive impairment in dementia [17]. Therefore, the cholinergic hypothesis has served as the basis for treatment in AD [18], and attempts to treat the cognitive dysfunction in AD have been focused on enhancing the cholinergic

function through AChE inhibitors [19]. AChE inhibitors in AD therapy should boost endogenous levels of ACh in the brain and thereby enhance the cholinergic neurotransmission. Several AChE inhibitors are now used for the symptomatic treatment of AD. Functional imaging of cholinergic neurotransmission is a useful strategy for the determination of the treatment protocol of demented patients. The use of tracers that are hydrolyzed specifically by AChE permits the measurement and imaging of local AChE activity in humans [20]. Clinical PET studies using [^{11}C]MP4A and [^{11}C]PMP indicated that AChE activity is prominently reduced in AD [21,22]. A recent [^{11}C]MP4A PET study demonstrated further significant reduction of AChE activity in the medial occipital cortex of PD and DLB patients [23]. The reduction of cortical k_3 value was greater in DLB patients (27.1%) than AD patients (13%), suggesting it might be useful in differentiating AD from DLB. The second approach to the evaluation of AChE function is using the AChE inhibitors themselves as radiotracers. This method enables a direct investigation of the pharmacokinetics of AChE inhibitors using PET. Donepezil hydrochloride is at present the AChE inhibitor most widely used for the treatment of AD and shows a selective binding of AChE compared with butyrylcholinesterase [24]. Radiolabeled donepezil can thus be used as a tracer to measure the concentration of brain AChE *in vivo*. A [^{11}C]donepezil PET study clearly revealed higher concentrations of tracer distribution in the striatum and cerebellum than in the neocortex and a prominent reduction of donepezil binding in the brains of AD patients [25]. The correlation of donepezil binding with severity of dementia was observed with AD patients. The amount of therapeutic drug bound to AChE is considered to be a key factor in determining the treatment response in each patient. A post-treatment PET study following the administration of 5 mg donepezil a day revealed an ~ 60% reduction of [^{11}C]donepezil binding throughout the brain [25]. This finding indicates that the AChE occupancy by orally administered donepezil was ~ 40% in daily doses of 5 mg. A [^{11}C]MP4A PET study revealed a mean 39% reduction in AChE activity after oral administration of 3 – 5 mg donepezil [26]. These findings together suggest that inhibition of AChE activity matches occupancy of AChE inhibitor binding sites. The *in vivo* evaluation of AChE occupancy using [^{11}C]donepezil PET could thus be a powerful strategy for determining the optimal dose of donepezil in AD therapy. Nicotinic ACh receptors have also been implicated in a variety of central processes, such as memory and cognition [27,28]. Abnormally low densities of nicotinic ACh receptors have been measured *in vitro* in autopsy brain tissue of AD patients [29]. Only PET studies using [^{11}C]nicotine found reduced uptake and binding in the temporal and frontal cortices of AD patients [28]. However, a recent PET study using 2-[^{18}F]fluoro-A-85380 found no evidence of *in vivo* nicotinic ACh receptor loss in early AD despite significant cognitive impairment [30]. Although the main focus of

neuroreceptor studies in AD has been the study of nicotinic ACh receptors, muscarinic ACh receptors, especially the M1 and M2 muscarinic ACh receptors subtypes, have also been implicated in AD [31]. Highly selective subtype-specific radioligands for M1 or M2 muscarinic ACh receptors are not yet available [32], but radiotracers that can assist in both quantifying muscarinic ACh receptor densities and monitoring AD therapy are being developed [33].

One of the major neuropathological findings in DLB is the loss of dopaminergic neurons in the substantia nigra. Such neuronal loss can be quantified by assessing striatal dopaminergic terminals with PET or SPECT, using ligands specific for the dopamine transporter, such as [¹²³I]-β-CIT and [¹²³I]FPCIT [34,35]. The evaluation of presynaptic dopamine synthesis by [¹⁸F]FDOPA PET demonstrated a prominent reduction in striatal accumulation in DLB patients [36], while the assessment of striatal dopaminergic terminals with vesicular monoaminergic transporter type 2 (VMAT2) tracers is also useful in distinguishing AD from DLB [37], suggesting that the assessment of the nigrostriatal dopaminergic function using PET and SPECT would be an informative diagnostic adjunct in distinguishing DLB from other types of neurodegenerative dementia. Another strategy to gain an accurate differential diagnosis of DLB from AD is the assessment of the cardiovascular autonomic dysfunction using scintigraphy with [¹²³I]metaiodobenzylguanidine (MIBG). This tracer enables the quantification of the post-ganglionic cardiac sympathetic innervation. Several studies using [¹²³I]MIBG scintigraphy have demonstrated a reduced cardiac retention compared with mediastinal uptake in DLB, as opposed to AD [38,39].

4. Imaging of neuroinflammation

Microglia are the primary resident immune surveillance cells in the brain and are thought to play a significant role in the pathogenesis of several neurodegenerative disorders, including AD [40]. *In vivo* measurement of microglial activation may help chart the progression of neuroinflammation as well as assess the efficacy of therapies designed to modulate neuroinflammation. Activated microglia can be measured using radioligands for the peripheral benzodiazepine receptor. [¹¹C]PK11195 has been widely used for this purpose in several neurodegenerative disorders. A recent PET study using [¹¹C]PK11195 demonstrated significant increase in microglial activation in AD brains and correlation of cortical microglial activation with the severity of dementia, which is compatible with a role of microglia in neuronal damage [41,42]. However, recent PET studies also indicated that cortical microglial activation measured by [¹¹C]PK11195 is not associated with amyloid deposition in the early stage of AD [43,44]. Despite its wide application, [¹¹C]PK11195 has a high lipophilicity and a high nonspecific binding, which makes it difficult to perform an accurate and sensitive measurement of microglial activation. Therefore, efforts are being made

to develop more sensitive radiotracers for the peripheral benzodiazepine receptor [45].

5. Imaging amyloid deposits in the brain

As mentioned before, the pathological hallmarks of AD are SPs and NFTs [46]. SPs are composed of amyloid-β (Aβ) protein. Aβ is a 4 kDa 39 – 43 amino acid metalloprotein derived from the proteolytic cleavage of the amyloid precursor protein (APP) by β- and γ-secretases. The abnormal accumulation of SPs has been implicated as the central event in the etiology and pathogenesis of AD [47] and precedes the cognitive decline observed in AD [48]. *In vivo* detection of SPs in the brain enables the identification of AD pathology even in subjects in their presymptomatic stage. A deeper understanding of the molecular mechanism of Aβ formation, degradation and neurotoxicity is being translated into new therapeutic approaches. The most promising approaches focus on reducing Aβ formation through β- and γ-secretase inhibitors or on increasing the removal of Aβ by immunotherapy or metal-protein attenuating compounds aimed at blocking the formation of Aβ oligomers and fibrils, inhibiting neurotoxicity [49,50]. For the assessment of preventive intervention and monitoring of therapeutic effects, it is desirable to measure non-invasively the amount of Aβ deposit in the living brain.

Although these Aβ deposits are still well beyond the resolution of conventional neuroimaging techniques, the density of these deposits in the brain tissue can be measured through specific radiotracer and nuclear medicine techniques. Many β-sheet binding agents have been developed as Aβ binding radiotracers for PET and SPECT imaging. The chemical structures of PET amyloid imaging agents are shown in Figure 1. The first compound to emerge as an amyloid-imaging agent was Chrysamine-G [51]. This compound shows similar binding characteristics as Congo Red but, unfortunately, its blood-brain barrier (BBB) permeability of Chrysamine-G is limited. Other derivatives including 1-bromo-2,5-bis-(3-hydroxycarbonyl-4-hydroxy) styrylbenzene (BSB), 1-iodo-2,5-bis-(3-hydroxycarbonyl-4-hydroxy) styrylbenzene (ISB), X-34 and methoxy X-04 have also been developed to improve BBB permeability [52-55]. Among them, BSB successfully visualized the brain amyloid deposits of APP transgenic mice after the intravenous administration of this compound. However, the BBB permeability of this agent was still inadequate to use as a clinical PET tracer. A marked progression in the development of amyloid-imaging tracers was the development of 2-(1-{6-[(2-[¹⁸F]fluoroethyl)(methyl)amino]-2-naphthyl} ethylidene)malononitrile([¹⁸F]FDDNP) [56,57]. This compound is highly lipophilic and can easily cross the BBB, and has been used in human PET studies. The [¹⁸F]FDDNP PET scan successfully differentiated people with AD and MCI from those with no cognitive impairment [58]. This agent has some limitations in its practical use owing to its low signal-to-background ratio. Direct comparison of [¹⁸F]